

Moving Beyond Sparse Grounding with Complete Screen Parsing Supervision

A. Said Gurbuz^{1,2} Sunghwan Hong^{*2,3,4} Ahmed Nassar¹ Marc Pollefeys² Peter Staar¹

Abstract

Modern computer-use agents (CUA) must perceive a screen as a structured state, what elements are visible, where they are, and what text they contain, before they can reliably ground instructions and act. Yet, most available grounding datasets provide sparse supervision, with *insufficient* and *low-diversity* labels that annotate only a small subset of task-relevant elements per screen, which limits both coverage and generalization; moreover, practical deployment requires efficiency to enable low-latency, on-device use. We introduce **ScreenParse**, a large-scale dataset for *complete* screen parsing, with dense annotations of all visible UI elements (boxes, 55-class types, and text) across 771K web screenshots (21M elements). ScreenParse is generated by **Webshot**, an automated, scalable pipeline that renders diverse urls, extracts annotations and applies VLM-based relabeling and quality filtering. Using ScreenParse, we train **ScreenVLM**, a compact, 316M-parameter vision language model (VLM) that decodes a compact ScreenTag markup representation with a structure-aware loss that upweights structure-critical tokens. ScreenVLM substantially outperforms much larger foundation VLMs on dense parsing (e.g., 0.592 vs. 0.294 PageIoU on ScreenParse) and shows strong transfer to public benchmarks. Moreover, finetuning foundation VLMs on ScreenParse consistently improves their grounding performance, suggesting that dense screen supervision provides transferable structural priors for UI understanding. Project page: <https://saidgurbuz.github.io/screenparse/>.

1. Introduction

The rise of vision language models has opened a new era of computer use agents capable of interacting with graphical user interfaces (GUI) to perform complex tasks (Wang et al., 2025a; Qin et al., 2025; He et al., 2024; Zhang et al., 2025). Despite rapid progress, a fundamental bottleneck persists: the *grounding* problem (Cheng et al., 2024; Feizi et al., 2025). To operate effectively, a screen agent must first accurately identify UI elements, understand their roles, and reason about their spatial and functional relationships. This structural understanding is a prerequisite for effective downstream planning and action execution; when it fails, errors cascade throughout the agent pipeline.

Current state-of-the-art models for GUI interaction predominantly rely on “sparse” action-oriented datasets that annotate only the single element relevant to each task step (Deng et al., 2023; Zhou et al., 2024; Rawles et al., 2023; Xie et al., 2024). Such supervision is valuable for end-to-end policies, but it leaves the majority of on-screen elements unlabeled and the full screen structure implicit. As a result, models can learn shortcuts that are sufficient for the supervised steps while failing to form a complete screen state, which can hurt robustness and generalization to new layouts, applications, and out-of-distribution screens. In addition, practical deployments often require low-latency, on-device inference, motivating compact perception models rather than relying exclusively on large foundation VLMs (Bai et al., 2025; Zhu et al., 2025).

We argue that a natural remedy is to treat **complete screen parsing** as a core training objective. We define screen parsing as recovering the complete semantic structure of a screen: the set of all visible UI elements, their bounding boxes, semantic types, and associated text. Compared to single-target grounding, dense screen parsing provides a holistic screen understanding that downstream agents can condition on for instruction following and action selection.

A key challenge is that dense, complete annotations are expensive to obtain by human annotators and difficult to maintain at scale, especially on the web where pages are dynamic and Document Object Model (DOM)-derived elements can be noisy, redundant, or visually irrelevant. To address this, we introduce **Webshot**, a scalable pipeline that renders diverse web pages and extracts dense DOM-aligned

¹IBM Research Zurich, Zurich, Switzerland ²ETH Zurich, Computer Vision and Geometry (CVG), Switzerland ³ETH AI Center, Switzerland ⁴ETH Zurich, Photogrammetry and Remote Sensing (PRS), Switzerland. Correspondence to: Sunghwan Hong* <sunghwan.hong@ai.ethz.ch>.

UI annotations, then applies VLM-based refinement and quality filtering to produce a high-quality dataset. Fig. 3 summarizes the Webshot pipeline.

Leveraging our Webshot pipeline, we construct **ScreenParse**, a large-scale dataset for complete screen parsing that provides dense annotations for all visible UI elements, including their bounding boxes, semantic types, and text, spanning 55 UI categories. Building on this data, we train **ScreenVLM**, an ultra-lightweight vision–language model that parses full screens into a structured sequence representation, ScreenTag. To better align optimization with structured extraction, we further introduce a structure-aware weighted loss that upweights structure-critical tokens *e.g.*, tags and locations, improving the fidelity of predicted layouts.

Empirically, ScreenVLM substantially outperforms much larger foundation VLM baselines on dense parsing and transfers effectively to public benchmarks. Moreover, we demonstrate that ScreenParse supervision benefits other model families as well, strengthening both foundational VLMs and detector-based parsers. These results suggest that dense screen supervision provides transferable structural priors for robust UI understanding.

In summary, our key contributions are:

- We introduce **ScreenParse**, a large-scale dataset for *complete* screen parsing, providing dense annotations of all visible UI elements, such as bounding boxes, element types, and text, across 55 UI categories.
- We propose **Webshot**, a scalable and fully automated pipeline that collects dense, hierarchy-preserving screen parsing annotations from rendered web pages.
- We show that training on **ScreenParse** yields strong and transferable gains: our proposed **ScreenVLM** architecture, as well as existing foundation VLMs and state-of-the-art detector-based parsers, improve substantially on both our benchmark and public UI understanding benchmarks.

2. Related Work

Computer-Use Agents and Evaluation. Recent benchmarks evaluate end-to-end agents that perceive screens and execute actions in web and OS environments, spanning interactive tasks and demonstration-based settings (Zhou et al., 2024; Koh et al., 2024; He et al., 2024; Xie et al., 2024; Deng et al., 2023). More recent suites (Wang et al., 2025b) further expand evaluation to structured, multi-platform protocols. Although critical for assessing long-horizon success, these benchmarks often leave a fine-grained perception implicit; our work targets this gap by enabling dense screen-level supervision for both training and evaluation.

UI Grounding Benchmarks and Datasets. A closely related line of work studies UI grounding, where models localize elements referred to by natural-language instructions. SeeClick and ScreenSpot/ScreenSpotPro popularize instruction-conditioned grounding evaluation, and a concurrent work, GroundCUA, provides more complete screen-level annotations derived from human demonstrations (Cheng et al., 2024; Li et al., 2025; Feizi et al., 2025). However, most benchmarks offer sparse supervision (one instruction to one or a few elements), while more complete datasets like GroundCUA are limited in scale and diversity. In contrast, our dataset targets *complete* screen parsing with dense annotations of nearly all visible UI elements after rendering, providing a holistic perception prior that complements instruction-level grounding.

Foundation VLMs and Parsers. Foundation VLMs, such as Qwen3-VL, InternVL3, and Gemini-2.5, can be prompted for various downstream applications (Yoon et al., 2025; Han et al., 2025). Apart from them, grounding and structured extraction are common baselines for GUI perception (Bai et al., 2025; Zhu et al., 2025; Comanici et al., 2025). In parallel, specialized parsers such as OmniParser localize UI elements via detector-based pipelines (Lu et al., 2024). In practice, foundation VLMs are often too large for low-latency or on-device deployment, while detector-style parsers focus on localization and lack language-grounded structured understanding for downstream reasoning. Our work bridges this gap by using dense supervision to train an ultra-compact VLM for complete screen parsing, and we further show that the same supervision improves both foundation VLMs and detector-based parsers on our benchmark and public evaluations (Feizi et al., 2025; Cheng et al., 2024).

3. Dataset: ScreenParse

3.1. Overview

This section introduces *ScreenParse*, a web-scale dataset for *complete screen parsing*, the task of recovering all rendered visible UI elements on a screen together with their locations, semantic types, and text. Unlike most GUI agent and grounding datasets that provide sparse supervision for only the interacted or instruction-referred element(s) (Deng et al., 2023; Zhou et al., 2024; Rawles et al., 2023; Cheng et al., 2024; Xie et al., 2024), ScreenParse provides dense, screen-level annotations that encourage holistic screen understanding and make it possible to train parsers that generalize across diverse layouts.

ScreenParse contains **771K** rendered webpage screenshots with **21M** UI element annotations spanning **55** classes. Importantly, it includes both fine-grained atomic elements and semantically meaningful container elements, enabling models to learn hierarchical structure beyond isolated bound-

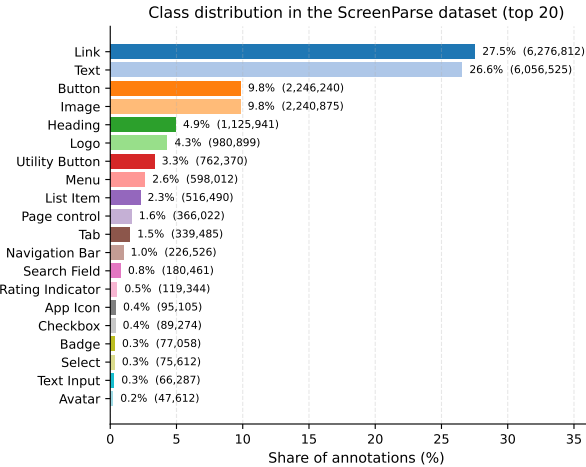


Figure 1. Class distribution of the top-20 most frequent UI elements in the *ScreenParse* dataset.

Table 1. Statistics of the *ScreenParse* dataset.

Split	Images	Annotations
Train	693,975	18,968,147
Val	38,850	1,062,552
Test	38,633	1,063,544
Total	771,458	21,094,243

ing boxes. We split the dataset into train/val/test using a **90/5/5%** split; Tab. 1 reports split sizes, and Fig. 1 shows the class distribution of the most frequent UI types.

Comparison to Prior Datasets. Tab. 2 contrasts ScreenParse with representative GUI grounding datasets. We mark a dataset as *complete annotation* if it labels (approximately) *all visible UI elements per screen*, rather than only task-relevant or instruction-referred elements. ScreenParse provides complete annotations at substantially larger scale and with a more fine-grained label taxonomy, while preserving hierarchical structure through container elements. This makes ScreenParse particularly suited for pre-training and evaluating models that aim to build holistic screen understanding, and also provides a strong supervision source for training detector-based parsers under a unified taxonomy. Next, we describe Webshot in detail.

3.2. Dataset Pipeline: Webshot

ScreenParse is generated entirely by our automated **Webshot** pipeline, which renders diverse URLs, extracts DOM-aligned candidates, and applies refinement and quality filtering to produce high-coverage dense annotations at scale without human intervention. An overview of the Webshot pipeline is visualized in Fig. 3.

Web Crawling. To begin with, we collect a diverse set of web page screenshots by crawling **1 million** unique URLs

Table 2. Comparison of grounding datasets. *Complete annotation* indicates whether all visible UI elements on each screen are labeled (dense), as opposed to only a sparse subset (e.g., task-relevant or instruction-referred elements). #E and #S denote the numbers of labeled elements and samples, respectively. ^{*}These datasets do not define a well-specified set of UI element types.

Grounding Dataset	Complete annotation	# of types	Scale	
			# of E	# of S
UGround (Gou et al., 2025)	✗	1	9M	773k
JEDI (Xie et al., 2024)	✗	4	4M	575k
AGUVIS-G (Xu et al., 2025)	✗	1	3.8M	452k
OS-ATLAS (Wu et al., 2025)	✗	1 [*]	14.5M	1.85M
RICOSCA (Deka et al., 2017)	✗	1 [*]	170K	18K
UIBERT (Bai et al., 2021)	✗	32	166K	57K
Widget Caption (Li et al., 2020)	✗	1	101K	14K
AMEX (Chai et al., 2025)	✗	2	1.2M	101K
ScreenSpot (Cheng et al., 2024)	✗	2	3M	270K
GroundCUA (Feizi et al., 2025)	✓	8	3.56M	55k
ScreenParse (Ours)	✓	55	21M	771k



Figure 2. Qualitative example from *ScreenParse* illustrating dense, complete UI annotations visualized as labeled bounding boxes.

from the public *45 Million Websites dataset*¹. This dataset aggregates URLs from multiple sources, including Common Crawl, Alexa Top Sites, and public domain lists. We then curate a balanced subset of URLs spanning various categories (e.g., e-commerce, news, social media, blogs) to ensure diversity in layout and content.

Annotation Pipeline: Bounding Box Extraction and Filtering. To obtain dense, screen-complete annotations, we render each URL with Playwright² and capture full-page screenshots. For each rendered page, we extract the DOM tree along with associated metadata, then apply cleaning and visibility-based filtering to retain on-screen elements: we remove degenerated boxes and elements with negligible visible area in the rendered viewport, *e.g.*, off-screen/hidden/tiny artifacts, and suppress near-duplicate overlapping boxes introduced by nested DOM wrappers. This yields, per screenshot, bounding boxes, class labels, and text content for all visible UI elements. Crucially, we

¹https://huggingface.co/datasets/PlugiloInc/45_Million_Worlds

²<https://github.com/microsoft/playwright>

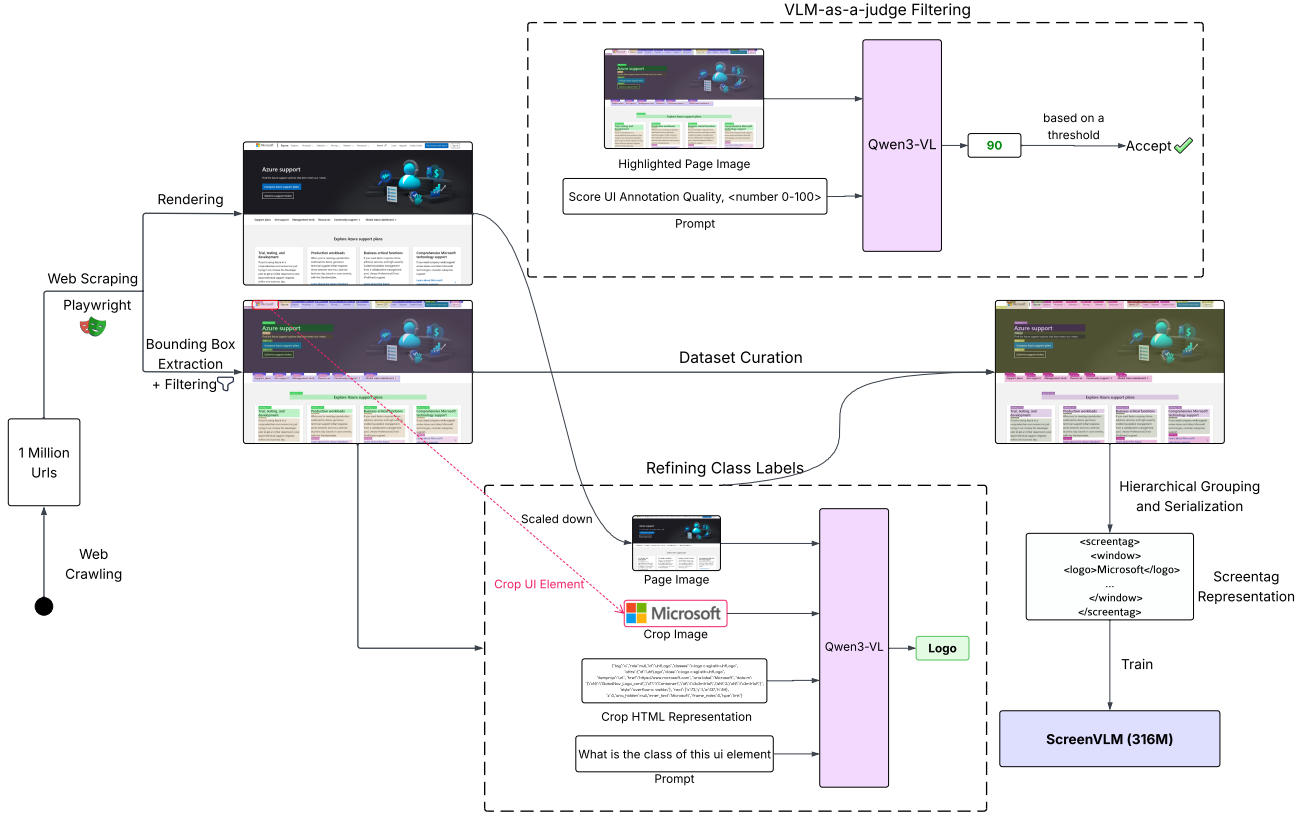


Figure 3. Overview of the Webshot dataset generation pipeline. Our scalable framework renders diverse URLs with Playwright and extracts DOM-driven dense annotations. VLMs further refine UI element types and filter low-quality samples.

preserve the DOM hierarchy: in addition to leaf nodes, we annotate enclosing container elements that carry semantic structure *e.g.*, navigation bars, cards, and modals. See Appendix 7.6 for details. Fig. 2 shows an example of the highlighted sample from ScreenParse.

Annotation Schema. We defined a taxonomy of **55** UI element classes based on common web design patterns from apple human interface guidelines, Material UI, and Fluent UI design systems (Apple, 2026; MUI, 2026; Microsoft, 2026). The full list of UI element classes is provided in the Appendix Tab. 8.

Label Refinement and Filtering. While the heuristic DOM-based labeling step (described above) provides broad coverage, it can be noisy due to heterogeneous and inconsistent markup in real-world web pages. We therefore refine labels with a VLM, using Qwen-3-VL-8B-Instruct (Bai et al., 2025). For each element, we input the full-page screenshot, the element crop, and a compact attribute representation, and prompt the model to predict one of the 55 UI classes. To further suppress noise from dynamic content, ads, and rendering artifacts, we apply a VLM-as-a-judge filter: for each page, we visualize all extracted boxes as an overlay and ask the model to score annotation quality (coverage,

false positives, duplicates, and localization). Pages below a quality threshold are discarded. Finally, we perform targeted human validation on held-out samples to calibrate thresholds and ensure label quality. Prompts for both refinement and filtering are provided in Appendix 7.7 and 7.8.

4. Method

4.1. Problem Formulation

Given a screenshot $I \in \mathbb{R}^{H \times W \times 3}$, screen parsing aims to recover the full set of visible UI elements together with their geometry, semantic type, and text content. Concretely, we represent a screen as a set of elements $S = \{e_i\}_{i=1}^N$ where each element $e_i = (b_i, c_i, t_i)$ consists of a bounding box $b_i = (x_1, y_1, x_2, y_2)$, a class label c_i from a fixed UI taxonomy, and optional visible text t_i . Unlike single-target grounding, the goal is to predict *all* elements on the screen, including fine-grained widgets and semantically meaningful containers, enabling holistic screen understanding.

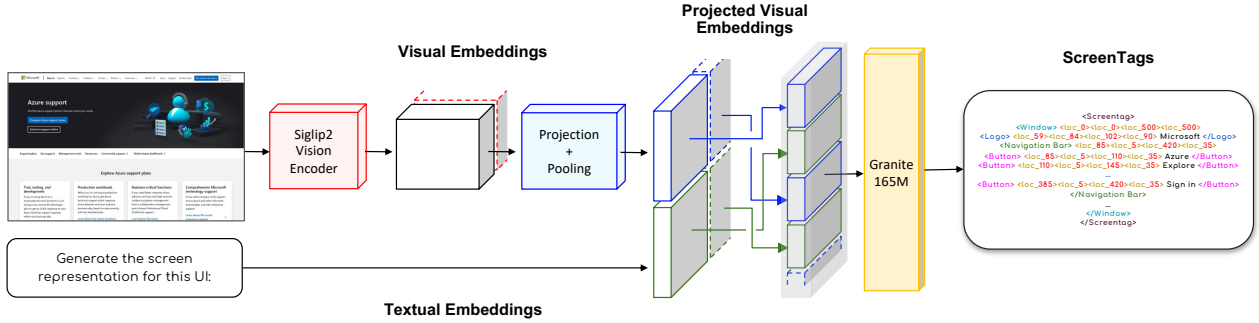


Figure 4. Overview of the ScreenVLM architecture. A screenshot is encoded by the SigLIP-2 vision encoder (Tschanne et al., 2025) into patch tokens, which are projected and fed to the Granite-165M LLM (Mishra et al., 2024) decoder together with text tokens to generate the ScreenTag sequence.

4.2. ScreenTag: Compact Screen Structure Representation

To train an autoregressive model for dense parsing, we serialize the screen into a compact xml-like structured sequence we call *ScreenTag*, inspired by OTSL (Lysak et al., 2023) and its successor DocTags (Nassar et al., 2025). Each element is emitted as a typed tag followed by discretized location tokens and optional text, and may include its serialized children:

```
<tag> <x1> <y1> <x2> <y2>
  [text] [children] </tag>
```

Coordinates are normalized and quantized to a **0-500** grid to balance spatial precision and vocabulary size. This representation is compact and unambiguous to parse from the model output, and it aligns naturally with autoregressive decoding for dense screen parsing.

4.3. Lightweight Vision-Language Model

ScreenVLM. ScreenVLM is a compact vision–language model that converts a screenshot into a serialized, structured screen representation (*ScreenTag*; Fig. 4). Rather than introducing a heavy new architecture, we adapt a document-to-markup VLM, *Granite Docling*, which is based on the Idefics3 family (Laurençon et al., 2024) and closely related to SmolDocling (Nassar et al., 2025), to the UI domain. Concretely, ScreenVLM couples a strong but efficient visual backbone (Tschanne et al., 2025), specialized in multimodal downstream tasks (Shin et al., 2024; Cho et al., 2024; Kim et al., 2025) with a lightweight Granite 165M autoregressive decoder (Mishra et al., 2024). The image is encoded into a small set of visual tokens that condition the decoder to generate ScreenTag sequences via standard autoregressive training. We initialize from a pretrained Granite Docling checkpoint, since its document conversion pretraining emphasizes localization-aware, structured extraction through markup-like outputs, an inductive bias that transfers naturally to complete screen parsing.

Training Objective. A standard sequence cross-entropy treats all tokens equally. However, in screen parsing, *structure* tokens–element types and locations—are far more consequential: small mistakes in tags or box coordinates can invalidate an element even if its text is correct. In addition, text tokens often dominate the sequence length, skewing optimization toward transcription rather than localization and typing. To emphasize structural fidelity, we adopt a structure-aware weighted cross-entropy over the ground-truth ScreenTag sequence:

$$\mathcal{L}(\theta) = - \sum_{t=1}^T w(y_t) \log p_\theta(y_t | y_{<t}, I),$$

$$w(y_t) = \begin{cases} \lambda_{\text{tag}} & y_t \in \mathcal{V}_{\text{tag}}, \\ \lambda_{\text{loc}} & y_t \in \mathcal{V}_{\text{loc}}, \\ 1 & \text{otherwise,} \end{cases} \quad (1)$$

where \mathcal{V}_{tag} and \mathcal{V}_{loc} denote the ScreenTag and location token sets, respectively.

5. Experiments

5.1. Implementation details.

We fine-tune ScreenVLM on the ScreenParse training split for **287,500** steps using **16** NVIDIA H100 GPUs (2 nodes \times 8 GPUs) with an effective batch size of **64**. We use parameter-group learning rates: 2.12×10^{-2} for the multi-modal projection (MP) layers and 2×10^{-3} for the vision and language backbones. Sequences are truncated or padded to a maximum length of 8192 tokens. Additional hyperparameters are in Appendix 7.2.

5.2. Experimental Setting

We evaluate three questions: (i) whether dense supervision enables accurate *complete screen parsing* in-domain, (ii) whether the resulting perception transfers to public

out-of-distribution GUI benchmarks, and (iii) whether our structure-aware loss improves parsing accuracy and transfer.

Datasets. We report results on: **ScreenParse** (in-domain dense parsing; 38.6K test screenshots), **GroundCUA** (Feizi et al., 2025) (OOD GUI screenshots across 87 software platforms; 55K screenshots, evaluated on the full benchmark), and **ScreenSpot** (Cheng et al., 2024) (sparse grounding across Web/PC/Mobile; 610 test samples total: 199 Web, 210 PC, 201 Mobile). Since these datasets use different label spaces, we evaluate with dataset-specific label vocabularies (details in Appendix 7.9).

Evaluation Metrics. We measure dense screen parsing quality using *PageIoU* (Niu et al., 2025), which compares the pixel coverage of the union of predicted boxes against the union of ground-truth boxes, capturing how completely a method recovers the screen layout. *Label PageIoU* is the label-aware variant that additionally requires the predicted element type to match the ground truth. We also report *Recall@50*, the fraction of ground-truth elements matched by a prediction with $\text{IoU} \geq 0.5$ (and matching class when labels are available), and *mAP@50* for models that provide confidence-ranked detections. For ScreenSpot, which provides sparse target annotations rather than full screens, we report *Recall@50* and *PixCov*, the fraction of annotated target pixels covered by predictions. The formal definitions are given in Appendix 7.3.

Evaluation protocol. We evaluate dense parsing on ScreenParse using *PageIoU*, *Label PageIoU*, *Recall@50*, and (when applicable) *mAP@50*. For GroundCUA, we evaluate on the full benchmark and report *PageIoU*/*Label PageIoU* to measure transfer to real, multi-application UI screenshots. For ScreenSpot (Web/PC/Mobile), we report *Recall@50* and *PixCov* to reflect performance under sparse element annotations. For VLM baselines, we run inference using vLLM (Kwon et al., 2023) with the fixed prompt templates in Appendix 7.9.

5.3. Baselines

We compare against two baseline families: (i) foundation VLMs for language-grounded structured extraction and (ii) detector-style UI parsers as strong, efficient localization backbones commonly used in agent pipelines.

VLM baselines. We evaluate Qwen3-VL-2B-Instruct, Qwen3-VL-8B-Instruct (Bai et al., 2025), and InternVL3-2B (Zhu et al., 2025). For each dataset, we prompt models to extract *all* visible UI elements and output bounding boxes, text, and labels constrained to the dataset taxonomy. We use a consistent prompting format across datasets; templates are provided in Appendix 7.9. To quantify the impact of dense ScreenParse supervision on foundation models, we addition-

Table 3. ScreenParse test set performance.

Model	Size	Page IoU	Label Page IoU	mAP@50
<i>VLMs</i>				
Qwen3-VL-8B-Instruct	8B	0.294	—	—
InternVL3-2B	2B	0.111	0.030	0.000
InternVL3-2B + ScreenParse	2B	0.509 <small>(+0.398)</small>	0.174 <small>(+0.144)</small>	0.072 <small>(+0.072)</small>
Qwen3-VL-2B-Instruct	2B	0.228	0.051	0.023
Qwen3-VL-2B-Instruct + ScreenParse	2B	0.585 <small>(+0.357)</small>	0.166 <small>(+0.115)</small>	0.152 <small>(+0.129)</small>
ScreenVLM (ours)	316M	0.606	0.197	0.303
<i>Detectors / Parsers</i>				
OmniParser V2	20M	0.270	—	—
OmniParser V2 + ScreenParse	20M	0.503	0.141	0.251
YOLO + ScreenParse	25M	0.533	0.133	0.299
RT-DETRv2 + ScreenParse	43M	0.600	0.172	0.362

Table 4. Performance on the GroundCUA dataset.

Model	Size	Page IoU	Label Page IoU
<i>VLMs</i>			
Qwen3-VL-8B-Instruct	8B	0.060	0.010
Qwen3-VL-2B-Instruct	2B	0.030	0.005
Qwen3-VL-2B-Instruct + ScreenParse	2B	0.090 <small>(+0.060)</small>	0.019 <small>(+0.014)</small>
InternVL3-2B	2B	0.025	0.006
InternVL3-2B + ScreenParse	2B	0.203 <small>(+0.178)</small>	0.036 <small>(+0.030)</small>
ScreenVLM (ours)	316M	0.251	0.043
<i>Detectors / Parsers</i>			
OmniParser V2	20M	0.361	0.049
OmniParser V2 + ScreenParse	20M	0.398	0.061
YOLO + ScreenParse	25M	0.379	0.057
RT-DETRv2 + ScreenParse	43M	0.388	0.059

ally fine-tune InternVL3-2B and Qwen3-VL-2B-Instruct on ScreenParse using ScreenTag format and evaluate them under the same inference protocol.

Detectors / parsers. We include OmniParser v2 (Lu et al., 2024), a widely used YOLO-based screen parser. Because it is not trained on our 55-class taxonomy, we primarily report class-agnostic localization metrics for its off-the-shelf outputs (e.g., *PageIoU* and *Recall@50*). To evaluate detector-style models under a unified taxonomy and measure how ScreenParse benefits this family, we (i) fine-tune OmniParser v2 on ScreenParse and (ii) train YOLOv11-large (Khanam & Hussain, 2024) and RT-DETRv2 (Lv et al., 2024) on the full 55-class label set.

5.4. Experimental Results

We evaluate ScreenVLM and ScreenParse along three axes: (i) in-domain dense parsing on ScreenParse, (ii) out-of-distribution transfer (GroundCUA and ScreenSpot), and (iii) ablation on our structure-aware loss.

In-domain dense parsing on ScreenParse. Tab. 3 reports results on the ScreenParse test set. Among VLMs, **ScreenVLM** achieves the strongest dense parsing quality despite being substantially smaller than prompted foundation VLM baselines. Benefiting from our initialization strategy (Sect. 4) and dense ScreenParse supervision, Screen-

Table 5. Performance on the ScreenSpot dataset across splits. Numbers under each split indicate # of samples / elements.

Model	Size	Web		PC		Mobile	
		Recall (199 / 436)	PixCov (199 / 436)	Recall (210 / 334)	PixCov (210 / 334)	Recall (201 / 502)	PixCov (201 / 502)
<i>VLMs</i>							
Qwen3-VL-8B-Instruct	8B	0.229	0.346	0.201	0.300	0.193	0.311
Qwen3-VL-2B-Instruct	2B	0.232	0.292	0.171	0.218	0.143	0.250
Qwen3-VL-2B-Instruct + ScreenParse	2B	0.477 (+0.245)	0.720 (+0.428)	0.201 (+0.030)	0.443 (+0.225)	0.108 (-0.035)	0.477 (+0.227)
InternVL3-2B	2B	0.002	0.057	0.018	0.109	0.068	0.321
InternVL3-2B + ScreenParse	2B	0.172 (+0.170)	0.592 (+0.535)	0.081 (+0.063)	0.628 (+0.519)	0.100 (+0.032)	0.527 (+0.206)
ScreenVLM (ours)	316M	0.557	0.746	0.222	0.839	0.066	0.847
<i>Detectors / Parsers</i>							
OmniParser V2	20M	0.541	0.629	0.483	0.557	0.489	0.521
OmniParser V2 + ScreenParse	20M	0.727	0.800	0.536	0.624	0.552	0.735
YOLO + ScreenParse	25M	0.683	0.798	0.521	0.597	0.504	0.682
RT-DETRv2 + ScreenParse	43M	0.768	0.857	0.590	0.699	0.584	0.736

VLM delivers strong parsing performance and surpasses much larger models. In particular, compared to Qwen3-VL-8B, ScreenVLM improves PageIoU from **0.294** to **0.606** and reaches Label PageIoU **0.197**, indicating better global coverage and more accurate label-aware structure recovery. InternVL3-2B and Qwen3-VL-2B perform substantially lower (PageIoU **0.111** and **0.228**, respectively). Overall, these results underscore the value of ScreenParse as dense supervision: prompted VLMs often miss many UI elements, whereas training with complete annotations yields markedly stronger recovery of screen structure.

Detection-based models trained on ScreenParse are also strong. RT-DETRv2 achieves PageIoU **0.600** and mAP@50 **0.362**, while YOLO achieves PageIoU **0.533** and mAP@50 **0.299**, which is expected given their detection-centric architectures. However, detectors do not produce a language-grounded screen state suitable for downstream instruction-conditioned reasoning or action generation. In contrast, ScreenVLM outputs a structured, language-aligned representation that unifies geometry, semantics, and text, making it a better fit as a pretrained model to be fine-tuned for computer-use tasks. We therefore report VLMs and detectors separately and interpret results in light of their respective strengths.

Transfer to GroundCUA. Tab. 4 evaluates transfer to GroundCUA, which contains UI screenshots from diverse applications and is out-of-distribution relative to our web-only ScreenParse training. Despite this shift, ScreenVLM remains the strongest VLM baseline, achieving PageIoU **0.251** and Label PageIoU **0.043**, compared to Qwen3-VL-8B at **0.060/0.010** and InternVL3-2B at **0.025/0.006**. This indicates that dense parsing supervision induces structural priors that transfer beyond the web domain.

Fine-tuning a foundation VLM on ScreenParse further im-

proves transfer: InternVL3-2B increases from **0.025/0.006** to **0.203/0.036**, narrowing the gap to ScreenVLM and supporting the view that dense screen parsing supervision is broadly beneficial rather than model-specific. Detector-based parsers obtain higher absolute localization scores on GroundCUA (e.g., OmniParser v2 fine-tuned reaches PageIoU **0.398**), consistent with specialization and the evaluation’s emphasis on box overlap. Importantly, ScreenVLM reduces the gap to detector pipelines while producing a structured, language-compatible output that is directly usable by downstream agents.

ScreenSpot: grounding-style evaluation under sparse annotations. Tab. 5 reports results on ScreenSpot (Web/PC/Mobile). Because ScreenSpot provides only sparse annotations, full-layout metrics such as PageIoU are not directly applicable; we therefore report Recall@50 and PixCov. On the Web split, ScreenVLM achieves Recall@50 **0.557** and PixCov **0.746**, while detector-style parsers attain higher recall (e.g., RT-DETRv2 Recall@50 **0.768**, PixCov **0.857**). On PC and Mobile, ScreenVLM’s Recall@50 drops to **0.222** and **0.066**, yet PixCov remains high at **0.839** and **0.847**. This discrepancy suggests that under out-of-distribution UI styles, ScreenVLM often predicts regions that cover annotated pixels (high PixCov) but fails to produce tight element-level boxes required by Recall@50, which is more sensitive to precise localization. Overall, the results indicate non-trivial transfer from ScreenParse supervision, while revealing a clear limitation and future direction: extending dense supervision beyond web pages to better match PC/Mobile UI distributions and improve element-level recall.

Dense Supervision improves Foundation VLMs. We further analyze whether ScreenParse benefits models beyond ScreenVLM by fine-tuning multiple foundation VLMs on ScreenParse and comparing against their pretrained coun-

Table 6. Ablation on ScreenVLM training loss. We compare standard cross-entropy (CE) against our structure-aware weighted loss on ScreenParse, GroundCUA, and ScreenSpot (Web/PC/Mobile). Recall denotes class-agnostic Recall@50.

Model	ScreenParse		GroundCUA		ScreenSpot (Web)	ScreenSpot (PC)	ScreenSpot (Mobile)
	Page IoU	Label Page IoU	Page IoU	Label Page IoU	Recall	Recall	Recall
ScreenVLM (CE)	0.592	0.192	0.226	0.039	0.541	0.129	0.052
ScreenVLM (StructureAware)	0.606 (+2.4%)	0.197 (+2.6%)	0.251 (+11.1%)	0.043 (+10.3%)	0.557 (+3.0%)	0.222 (+72.1%)	0.066 (+26.9%)

Table 7. Inference efficiency under vLLM on a single H100. Latency is mean \pm std over 128 samples.

Model	Size (MB)	Latency (ms) \downarrow	Throughput (s $^{-1}$) \uparrow
Qwen3-VL-2B-Instruct	4300	1289.1 \pm 251.7	0.78
InternVL3-2B	4178	1267.3 \pm 187.9	0.79
ScreenVLM (Ours)	632	276.4 \pm 139.0	3.62

terparts in Tabs. 3, 4, and 5 (see Appendix Tab. 9 for a summary). Across architectures, dense supervision yields consistent gains in both in-domain dense parsing and out-of-distribution transfer. For example, fine-tuning Qwen3-VL-2B improves ScreenParse PageIoU from **0.228** to **0.585**, Label PageIoU from **0.051** to **0.166**, and mAP@50 from **0.023** to **0.152**, and also improves GroundCUA PageIoU from **0.030** to **0.090**. On ScreenSpot, PixCov increases substantially across splits (e.g., Web **0.292** \rightarrow **0.720**, PC **0.218** \rightarrow **0.443**), indicating improved grounding under sparse annotations.

The same trend holds for a different model family: after fine-tuning, InternVL3-2B improves from **0.111** \rightarrow **0.509** PageIoU and **0.036** \rightarrow **0.174** Label PageIoU on ScreenParse, and from **0.025** \rightarrow **0.203** PageIoU and **0.006** \rightarrow **0.036** Label PageIoU on GroundCUA. Together, these results indicate that the benefit of ScreenParse is not model-specific: dense, screen-level supervision consistently strengthens holistic screen understanding and transfers to new UI domains, sometimes enabling a smaller fine-tuned foundation model to outperform a larger prompted counterpart.

More Qualitative Results. Additional qualitative results are provided in Appendix 7.5.

5.5. Ablation Study and Analysis

Ablation study on structure-aware loss improves robustness. To isolate the effect of our structure-aware objective, we train the same ScreenVLM architecture under identical settings with (i) standard cross-entropy and (ii) the structure-aware weighted loss from Eq. 1, and compare on ScreenParse, GroundCUA, and ScreenSpot.

Relative to standard cross-entropy, the structure-aware loss improves ScreenParse PageIoU **0.592** \rightarrow **0.606** and GroundCUA PageIoU **0.226** \rightarrow **0.251**, while also improving ScreenSpot Recall across splits (Web **0.541** \rightarrow **0.557**, PC **0.129** \rightarrow **0.222**, Mobile **0.052** \rightarrow **0.066**). These gains are

largest under distribution shift (especially ScreenSpot PC), consistent with the goal of emphasizing structure-critical tokens (tags and locations) over long OCR-heavy sequences (see Tab. 6).

Efficiency. Tab. 7 summarizes the efficiency comparison. ScreenVLM is substantially more practical to deploy: it achieves $\sim 4\times$ higher throughput while being $\sim 6\times$ smaller than 2B-scale VLMs. This efficiency makes ScreenVLM well suited for low-latency screen understanding in resource-constrained settings, improving real-world practicality for computer-use agents.

6. Conclusion

We presented **ScreenParse**, a web-scale dataset for *complete* screen parsing with dense UI element annotations (boxes, 55-class types, and text) generated by our automated Webshot pipeline. Using ScreenParse, we trained **ScreenVLM**, a compact VLM that predicts a structured screen state, and introduced a structure-aware objective that emphasizes structure-critical tokens. Across in-domain evaluation on ScreenParse and transfer to public benchmarks (GroundCUA and ScreenSpot) (Feizi et al., 2025; Cheng et al., 2024), ScreenVLM substantially outperforms prompted foundation VLM baselines, while fine-tuning multiple foundation VLMs and parsers on ScreenParse yields consistent improvements, supporting the value of dense screen-level supervision for holistic UI understanding.

Limitations. While we show that models trained on ScreenParse transfer reasonably well to other domains, ScreenParse is predominantly web-centric, inevitably leaving a domain gap to native desktop/mobile applications and UI toolkits. Moreover, although Webshot applies extensive filtering and refinement, DOM-driven extraction can still contain residual noise from dynamic content (e.g., ads, overlays) and rendering artifacts, which may affect a subset of annotations.

Future Work. A natural next step is to expand dense parsing supervision beyond web pages to cover native desktop/mobile UIs and richer interaction contexts. Another promising direction is to leverage screen-parsing-pretrained models as strong visual backbones for *vision-language-action* agents by fine-tuning them on downstream interaction tasks

(e.g., click/type/scroll). This would capitalize on the holistic, language-aligned screen state to improve grounding and decision making.

References

Apple. Human interface guidelines. <https://developer.apple.com/design/human-interface-guidelines>, 2026. Accessed: 2026-01-23.

Bai, C., Zang, X., Xu, Y., Sunkara, S., Rastogi, A., Chen, J., and Agüera y Arcas, B. Uibert: Learning generic multimodal representations for ui understanding. In Zhou, Z.-H. (ed.), *Proceedings of the Thirtieth International Joint Conference on Artificial Intelligence, IJCAI-21*, pp. 1705–1712. International Joint Conferences on Artificial Intelligence Organization, 8 2021. doi: 10.24963/ijcai.2021/235. URL <https://doi.org/10.24963/ijcai.2021/235>. Main Track.

Bai, S., Cai, Y., Chen, R., Chen, K., Chen, X., Cheng, Z., Deng, L., Ding, W., Gao, C., Ge, C., Ge, W., Guo, Z., Huang, Q., Huang, J., Huang, F., Hui, B., Jiang, S., Li, Z., Li, M., Li, M., Li, K., Lin, Z., Lin, J., Liu, X., Liu, J., Liu, C., Liu, Y., Liu, D., Liu, S., Lu, D., Luo, R., Lv, C., Men, R., Meng, L., Ren, X., Ren, X., Song, S., Sun, Y., Tang, J., Tu, J., Wan, J., Wang, P., Wang, P., Wang, Q., Wang, Y., Xie, T., Xu, Y., Xu, H., Xu, J., Yang, Z., Yang, M., Yang, J., Yang, A., Yu, B., Zhang, F., Zhang, H., Zhang, X., Zheng, B., Zhong, H., Zhou, J., Zhou, F., Zhou, J., Zhu, Y., and Zhu, K. Qwen3-vl technical report, 2025. URL <https://arxiv.org/abs/2511.21631>.

Chai, Y., Huang, S., Niu, Y., Xiao, H., Liu, L., Wang, G., Zhang, D., Ren, S., and Li, H. AMEX: Android multi-annotation expo dataset for mobile GUI agents. In Che, W., Nabende, J., Shutova, E., and Pilehvar, M. T. (eds.), *Findings of the Association for Computational Linguistics: ACL 2025*, pp. 2138–2156, Vienna, Austria, July 2025. Association for Computational Linguistics. ISBN 979-8-89176-256-5. doi: 10.18653/v1/2025.findings-acl.110. URL <https://aclanthology.org/2025.findings-acl.110/>.

Cheng, K., Sun, Q., Chu, Y., Xu, F., YanTao, L., Zhang, J., and Wu, Z. SeeClick: Harnessing GUI grounding for advanced visual GUI agents. In Ku, L.-W., Martins, A., and Srikumar, V. (eds.), *Proceedings of the 62nd Annual Meeting of the Association for Computational Linguistics (Volume 1: Long Papers)*, pp. 9313–9332, Bangkok, Thailand, August 2024. Association for Computational Linguistics. doi: 10.18653/v1/2024.acl-long.505. URL <https://aclanthology.org/2024.acl-long.505/>.

Cho, S., Shin, H., Hong, S., Arnab, A., Seo, P. H., and Kim, S. Cat-seg: Cost aggregation for open-vocabulary semantic segmentation. In *Proceedings of the IEEE/CVF Conference on Computer Vision and Pattern Recognition*, pp. 4113–4123, 2024.

Comanici, G., Bieber, E., Schaekermann, M., Pasupat, I., Sachdeva, N., et al. Gemini 2.5: Pushing the frontier with advanced reasoning, multimodality, long context, and next generation agentic capabilities, 2025. URL <https://arxiv.org/abs/2507.06261>.

Deka, B., Huang, Z., Franzen, C., Hirschman, J., Afergan, D., Li, Y., Nichols, J., and Kumar, R. Rico: A mobile app dataset for building data-driven design applications. In *Proceedings of the 30th Annual ACM Symposium on User Interface Software and Technology, UIST '17*, pp. 845–854, New York, NY, USA, 2017. Association for Computing Machinery. ISBN 9781450349819. doi: 10.1145/3126594.3126651. URL <https://doi.org/10.1145/3126594.3126651>.

Deng, X., Gu, Y., Zheng, B., Chen, S., Stevens, S., Wang, B., Sun, H., and Su, Y. Mind2web: Towards a generalist agent for the web. In *Thirty-seventh Conference on Neural Information Processing Systems Datasets and Benchmarks Track*, 2023. URL <https://openreview.net/forum?id=kiYqb03wqw>.

Feizi, A., Nayak, S., Jian, X., Lin, K. Q., Li, K., Awal, R., Lù, X. H., Obando-Ceron, J., Rodriguez, J. A., Chapados, N., Vazquez, D., Romero-Soriano, A., Rabbany, R., Taslakian, P., Pal, C., Gella, S., and Rajeswar, S. Grounding computer use agents on human demonstrations, 2025. URL <https://arxiv.org/abs/2511.07332>.

Gou, B., Wang, R., Zheng, B., Xie, Y., Chang, C., Shu, Y., Sun, H., and Su, Y. Navigating the digital world as humans do: Universal visual grounding for GUI agents. In *The Thirteenth International Conference on Learning Representations*, 2025. URL <https://openreview.net/forum?id=kxnoqaisCT>.

Han, J., Hong, S., Jung, J., Jang, W., An, H., Wang, Q., Kim, S., and Feng, C. Emergent outlier view rejection in visual geometry grounded transformers. *arXiv preprint arXiv:2512.04012*, 2025.

He, H., Yao, W., Ma, K., Yu, W., Dai, Y., Zhang, H., Lan, Z., and Yu, D. WebVoyager: Building an end-to-end web agent with large multimodal models. In Ku, L.-W., Martins, A., and Srikumar, V. (eds.), *Proceedings of the 62nd Annual Meeting of the Association for Computational Linguistics (Volume 1: Long Papers)*, pp. 6864–6890, Bangkok, Thailand, August 2024. Association for Computational Linguistics. doi: 10.18653/v1/2024.acl-long.505.

371. URL <https://aclanthology.org/2024.acl-long.371/>.

Khanam, R. and Hussain, M. Yolov11: An overview of the key architectural enhancements, 2024. URL <https://arxiv.org/abs/2410.17725>.

Kim, C., Shin, H., Hong, E., Yoon, H., Arnab, A., Seo, P. H., Hong, S., and Kim, S. Seg4diff: Unveiling open-vocabulary segmentation in text-to-image diffusion transformers. *arXiv preprint arXiv:2509.18096*, 2025.

Koh, J. Y., Lo, R., Jang, L., Duvvur, V., Lim, M., Huang, P.-Y., Neubig, G., Zhou, S., Salakhutdinov, R., and Fried, D. VisualWebArena: Evaluating multimodal agents on realistic visual web tasks. In Ku, L.-W., Martins, A., and Srikumar, V. (eds.), *Proceedings of the 62nd Annual Meeting of the Association for Computational Linguistics (Volume 1: Long Papers)*, pp. 881–905, Bangkok, Thailand, August 2024. Association for Computational Linguistics. doi: 10.18653/v1/2024.acl-long.50. URL <https://aclanthology.org/2024.acl-long.50/>.

Kwon, W., Li, Z., Zhuang, S., Sheng, Y., Zheng, L., Yu, C. H., Gonzalez, J. E., Zhang, H., and Stoica, I. Efficient memory management for large language model serving with pagedattention. In *Proceedings of the ACM SIGOPS 29th Symposium on Operating Systems Principles*, 2023.

Laurençon, H., Marafioti, A., Sanh, V., and Tronchon, L. Building and better understanding vision-language models: insights and future directions. *ArXiv*, abs/2408.12637, 2024. URL <https://api.semanticscholar.org/CorpusID:271947166>.

Li, K., ziyang, M., Lin, H., Luo, Z., Tian, Y., Ma, J., Huang, Z., and Chua, T.-S. Screenspot-pro: GUI grounding for professional high-resolution computer use. In *Workshop on Reasoning and Planning for Large Language Models*, 2025. URL <https://openreview.net/forum?id=XaKNDIAHas>.

Li, Y., Li, G., He, L., Zheng, J., Li, H., and Guan, Z. Widget captioning: Generating natural language description for mobile user interface elements. In *Proceedings of the 2020 Conference on Empirical Methods in Natural Language Processing (EMNLP)*, pp. 5495–5510, 2020.

Lu, Y., Yang, J., Shen, Y., and Awadallah, A. Omniparser for pure vision based gui agent, 2024. URL <https://arxiv.org/abs/2408.00203>.

Lv, W., Zhao, Y., Chang, Q., Huang, K., Wang, G., and Liu, Y. Rt-detrv2: Improved baseline with bag-of-freebies for real-time detection transformer, 2024. URL <https://arxiv.org/abs/2407.17140>.

Lysak, M., Nassar, A., Livathinos, N., Auer, C., and Staar, P. Optimized table tokenization for table structure recognition. In *Document Analysis and Recognition - ICDAR 2023: 17th International Conference, San José, CA, USA, August 21–26, 2023, Proceedings, Part II*, pp. 37–50, Berlin, Heidelberg, 2023. Springer-Verlag. ISBN 978-3-031-41678-1. doi: 10.1007/978-3-031-41679-8_3. URL https://doi.org/10.1007/978-3-031-41679-8_3.

Microsoft. microsoft/fluentui. <https://github.com/microsoft/fluentui>, 2026. Accessed: 2026-01-23.

Mishra, M., Stallone, M., Zhang, G., Shen, Y., Prasad, A., Soria, A. M., Merler, M., Selvam, P., Surendran, S., Singh, S., Sethi, M., Dang, X.-H., Li, P., Wu, K.-L., Zawad, S., Coleman, A., White, M., Lewis, M., Pavuluri, R., Koyfman, Y., Lublinsky, B., de Bayser, M., Abdelaziz, I., Basu, K., Agarwal, M., Zhou, Y., Johnson, C., Goyal, A., Patel, H., Shah, S. Y., Zerfos, P., Ludwig, H., Munawar, A., Crouse, M., Kapanipathi, P., Salaria, S., Calio, B., Wen, S., Seelam, S., Belgodere, B., Fonseca, C. A., Singhee, A., Desai, N., Cox, D. D., Puri, R., and Panda, R. Granite code models: A family of open foundation models for code intelligence. *CoRR*, abs/2405.04324, 2024. URL <https://doi.org/10.48550/arXiv.2405.04324>.

MUI. Material ui. <https://mui.com/material-ui/>, 2026. Accessed: 2026-01-23.

Nassar, A., Omenetti, M., Lysak, M., Livathinos, N., Auer, C., Morin, L., de Lima, R. T., Kim, Y., Gurbuz, A. S., Dolfi, M., and Staar, P. W. J. Smoldocling: An ultra-compact vision-language model for end-to-end multimodal document conversion. In *Proceedings of the IEEE/CVF International Conference on Computer Vision (ICCV)*, pp. 21972–21983, October 2025.

Niu, J., Liu, Z., Gu, Z., Wang, B., Ouyang, L., Zhao, Z., Chu, T., He, T., Wu, F., Zhang, Q., Jin, Z., Liang, G., Zhang, R., Zhang, W., Qu, Y., Ren, Z., Sun, Y., Zheng, Y., Ma, D., Tang, Z., Niu, B., Miao, Z., Dong, H., Qian, S., Zhang, J., Chen, J., Wang, F., Zhao, X., Wei, L., Li, W., Wang, S., Xu, R., Cao, Y., Chen, L., Wu, Q., Gu, H., Lu, L., Wang, K., Lin, D., Shen, G., Zhou, X., Zhang, L., Zang, Y., Dong, X., Wang, J., Zhang, B., Bai, L., Chu, P., Li, W., Wu, J., Wu, L., Li, Z., Wang, G., Tu, Z., Xu, C., Chen, K., Qiao, Y., Zhou, B., Lin, D., Zhang, W., and He, C. Mineru2.5: A decoupled vision-language model for efficient high-resolution document parsing, 2025. URL <https://arxiv.org/abs/2509.22186>.

Qin, Y., Ye, Y., Fang, J., Wang, H., Liang, S., Tian, S., Zhang, J., Li, J., Li, Y., Huang, S., Zhong, W., Li, K.,

Yang, J., Miao, Y., Lin, W., Liu, L., Jiang, X., Ma, Q., Li, J., Xiao, X., Cai, K., Li, C., Zheng, Y., Jin, C., Li, C., Zhou, X., Wang, M., Chen, H., Li, Z., Yang, H., Liu, H., Lin, F., Peng, T., Liu, X., and Shi, G. Ui-tars: Pioneering automated gui interaction with native agents. *CoRR*, abs/2501.12326, January 2025. URL <https://doi.org/10.48550/arXiv.2501.12326>.

Rawles, C., Li, A., Rodriguez, D., Riva, O., and Lillicrap, T. P. Androidinthewild: A large-scale dataset for android device control. In *Thirty-seventh Conference on Neural Information Processing Systems Datasets and Benchmarks Track*, 2023. URL <https://openreview.net/forum?id=j4b315kO1l>.

Shin, H., Kim, C., Hong, S., Cho, S., Arnab, A., Seo, P. H., and Kim, S. Towards open-vocabulary semantic segmentation without semantic labels. *Advances in Neural Information Processing Systems*, 37:9153–9177, 2024.

Tschannen, M., Gritsenko, A., Wang, X., Naeem, M. F., Alabdulmohsin, I., Parthasarathy, N., Evans, T., Beyer, L., Xia, Y., Mustafa, B., Hénaff, O., Harmsen, J., Steiner, A., and Zhai, X. Siglip 2: Multilingual vision-language encoders with improved semantic understanding, localization, and dense features. *arXiv preprint arXiv:2502.14786*, 2025.

Wang, X., Wang, B., Lu, D., Yang, J., Xie, T., Wang, J., Deng, J., Guo, X., Xu, Y., Wu, C. H., Shen, Z., Li, Z., Li, R., Li, X., Chen, J., Boyuan, Z., PEIHANG, L., Lei, F., Cao, R., Fu, Y., Shin, D., Shin, M., Jiarui, H., Wang, Y., Chen, J., Ye, Y., Zhang, D., Wang, Y., Wang, H., Yang, D., Zhong, V., Y.Charles, Yang, Z., and Yu, T. OpenCUA: Open foundations for computer-use agents. In *The Thirty-ninth Annual Conference on Neural Information Processing Systems*, 2025a. URL <https://openreview.net/forum?id=6iRZvJiC9Q>.

Wang, X., Wu, Z., Xie, J., Ding, Z., Yang, B., Li, Z., Liu, Z., Li, Q., Dong, X., Chen, Z., Wang, W., Zhao, X., Chen, J., Duan, H., Xie, T., Yang, C., Su, S., Yu, Y., Huang, Y., Liu, Y., Zhang, X., Zhang, Y., Yue, X., Su, W., Zhu, X., Shen, W., Dai, J., and Wang, W. Mmbenchgui: Hierarchical multi-platform evaluation framework for gui agents, 2025b. URL <https://arxiv.org/abs/2507.19478>.

Wu, Z., Wu, Z., Xu, F., Wang, Y., Sun, Q., Jia, C., Cheng, K., Ding, Z., Chen, L., Liang, P. P., and Qiao, Y. OS-ATLAS: Foundation action model for generalist GUI agents. In *The Thirteenth International Conference on Learning Representations*, 2025. URL <https://openreview.net/forum?id=n9PDAFNi8t>.

Xie, T., Zhang, D., Chen, J., Li, X., Zhao, S., Cao, R., Hua, T. J., Cheng, Z., Shin, D., Lei, F., Liu, Y., Xu, Y., Zhou, S., Savarese, S., Xiong, C., Zhong, V., and Yu, T. Osworld: Benchmarking multimodal agents for open-ended tasks in real computer environments. In Globerson, A., Mackey, L., Belgrave, D., Fan, A., Paquet, U., Tomczak, J., and Zhang, C. (eds.), *Advances in Neural Information Processing Systems*, volume 37, pp. 52040–52094. Curran Associates, Inc., 2024. doi: 10.52202/079017-1650. URL https://proceedings.neurips.cc/paper_files/paper/2024/file/5d413e48f84dc61244b6be550f1cd8f5-Paper-Datasets_and_Benchmarks_Track.pdf.

Xu, Y., Wang, Z., Wang, J., Lu, D., Xie, T., Saha, A., Sahoo, D., Yu, T., and Xiong, C. Aguvic: Unified pure vision agents for autonomous gui interaction, 2025. URL <https://arxiv.org/abs/2412.04454>.

Yoon, H., Jung, J., Kim, J., Choi, H., Shin, H., Lim, S., An, H., Kim, C., Han, J., Kim, D., et al. Visual representation alignment for multimodal large language models. *arXiv preprint arXiv:2509.07979*, 2025.

Zhang, C., Li, L., He, S., Zhang, X., Qiao, B., Qin, S., Ma, M., Kang, Y., Lin, Q., Rajmohan, S., Zhang, D., and Zhang, Q. UFO: A UI-focused agent for windows OS interaction. In Chiruzzo, L., Ritter, A., and Wang, L. (eds.), *Proceedings of the 2025 Conference of the Nations of the Americas Chapter of the Association for Computational Linguistics: Human Language Technologies (Volume 1: Long Papers)*, pp. 597–622, Albuquerque, New Mexico, April 2025. Association for Computational Linguistics. ISBN 979-8-89176-189-6. doi: 10.18653/v1/2025.nacl-long.26. URL <https://aclanthology.org/2025.nacl-long.26>.

Zhou, S., Xu, F. F., Zhu, H., Zhou, X., Lo, R., Sridhar, A., Cheng, X., Ou, T., Bisk, Y., Fried, D., Alon, U., and Neubig, G. Webarena: A realistic web environment for building autonomous agents. In *The Twelfth International Conference on Learning Representations*, 2024. URL <https://openreview.net/forum?id=oKn9c6ytLx>.

Zhu, J., Wang, W., Chen, Z., Liu, Z., Ye, S., Gu, L., Tian, H., Duan, Y., Su, W., Shao, J., et al. Internvl3: Exploring advanced training and test-time recipes for open-source multimodal models. *arXiv preprint arXiv:2504.10479*, 2025.

Table 8. ScreenTag screen parsing classes (55 total) used in our dataset generation and screen parsing experiments.

ID	Class	ID	Class	ID	Class
1	Table	20	Scroll	39	Bottom navigation
2	Column/Browser	21	Switch	40	Breadcrumb
3	Button	22	File Icon	41	Page control
4	Utility Button	23	Chart	42	Link
5	App Icon	24	Window	43	Menu
6	Navigation Bar	25	Screen	44	Pagination
7	Status Bar	26	List	45	Tab
8	Search Field	27	List Item	46	Search Bar
9	Toolbar	28	PopUp Menu	47	Date-Time picker
10	Tooltip	29	Steppers	48	Calendar
11	Video	30	Toggles	49	Text
12	Tab Bar	31	Text Input	50	Heading
13	Side Bar	32	Rating Indicator	51	Code snippet
14	Slider	33	Checkbox	52	Carousel
15	Picker	34	Radiobox	53	Notification
16	ContextMenu	35	Select	54	Logo
17	DockMenu	36	Avatar	55	Progress bar
18	EditMenu	37	Badge		
19	Image	38	Alert		

7. Appendix

7.1. Screen Parsing Label Set (ScreenTag)

Tab. 8 lists the 55 semantic classes used for screen parsing in our ScreenTag annotation schema.

7.2. Training Details

Qwen3-VL-2B-Instruct Finetuning. We fine-tune Qwen3-VL-2B-Instruct on ScreenParse with BF16 and DeepSpeed ZeRO-3 offload, updating only the multimodal LLM (vision tower and projector frozen). We use batch size 1 with gradient accumulation 4, using AdamW optimizer with cosine schedule (3% warmup), learning rate 2×10^{-5} , weight decay 0.01, max sequence length 8192, and train for 5 epochs.

InternVL3-2B Finetuning. We fine-tune InternVL3-2B on ScreenParse using BF16 and DeepSpeed (ZeRO stage 1), freezing the vision backbone while updating the LLM and MLP. We train for 5 epochs with total batch size 128 (8 GPUs, batch size 4 per GPU, gradient accumulation 4), AdamW with cosine schedule (3% warmup), learning rate 2×10^{-5} , weight decay 0.05, and max sequence length 8192 with gradient checkpointing.

RT-DETRv2 Training. We train RT-DETRv2 with a PResNet-50-VD backbone, HybridEncoder, and RTDETRTransformerv2 on our COCO-format dataset (55 classes). Training uses total batch size 128 (val 64), images resized to 736×1280 , and augmentations including photometric distort, zoom-out, IoU crop, and random horizontal flip; heavy augmentations and multiscale are disabled after epoch 71. We optimize with AdamW (lr 8×10^{-4} , betas 0.9/0.999, weight decay 1×10^{-4}), using a lower backbone LR (8×10^{-5}) and zero weight decay for encoder/decoder norm/bn. We train for 72 epochs with linear warmup for 2000 iterations and a MultiStepLR (milestone 1000, gamma 0.1), and clip gradients at 0.1.

YOLOv11-L Training. We train a YOLOv11-L on the ScreenParse for 500 epochs at 1280 resolution with batch size 48 on 8 GPUs. We use AdamW with cosine learning-rate schedule ($1r0 = 2.08 \times 10^{-4}$, $1rf = 0.05$), momentum 0.9, weight decay 5×10^{-4} , and a short warmup (≈ 0.5 epochs) with patience of 25 epochs. We disable heavy composition augmentations (mosaic/mixup) and instead use mild geometric/color jitter with multi-scale training.

OmniParser v2 Finetuning. We fine-tune OmniParser v2 using the same training setup and augmentation configuration as our YOLOv11-L training, changing only the optimization schedule: we train for 100 epochs (vs. 500), use a higher base learning rate $1r0 = 2 \times 10^{-3}$ (vs. 2.08×10^{-4}), and set early-stopping patience to 20 (vs. 25).

For the structure-aware loss in Eq. 1 we set $\lambda_{\text{tag}} = 2$ and $\lambda_{\text{loc}} = 2$.

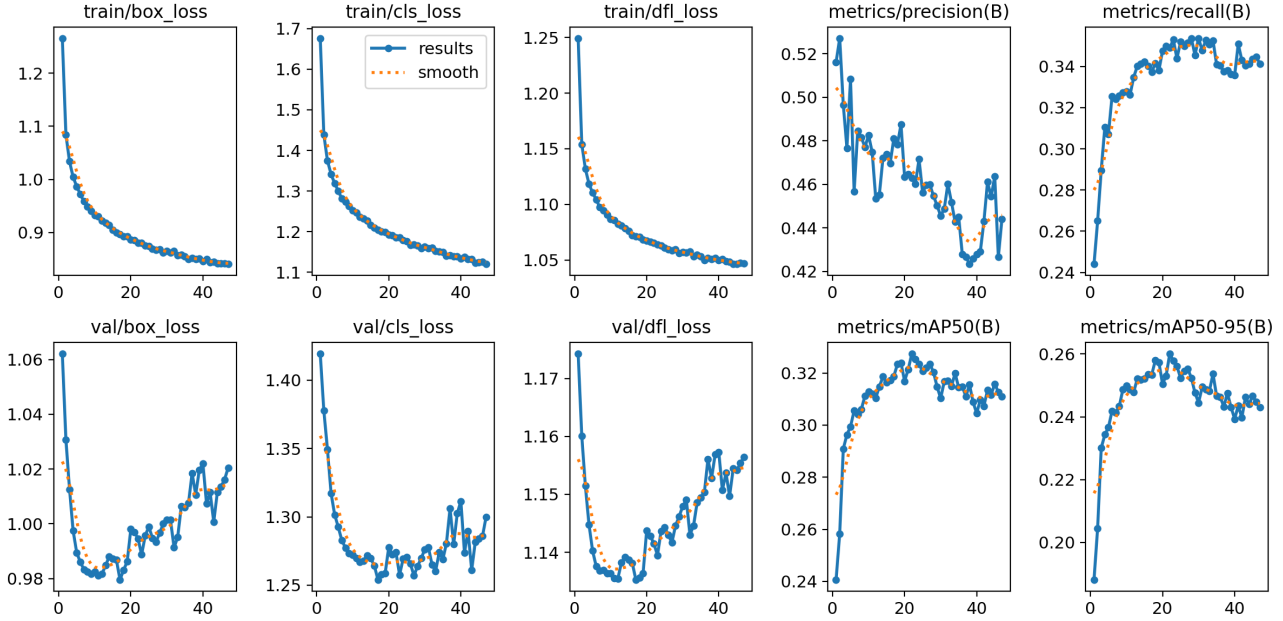


Figure 5. Training/Validation loss and accuracy curves for the YOLO component.

7.3. Evaluation Metrics

We use the indicator function $\mathbf{1}[\cdot]$, defined as $\mathbf{1}[s] = 1$ if statement s is true and 0 otherwise.

Let G be the set of ground-truth boxes and P the set of predicted boxes for an image with pixel domain Ω .

PageIoU. We define occupancy masks over pixels:

$$M_G(p) = \mathbf{1}[\exists g \in G \text{ s.t. } p \in g], \quad (2)$$

$$M_P(p) = \mathbf{1}[\exists b \in P \text{ s.t. } p \in b]. \quad (3)$$

PageIoU measures layout-level overlap between the unions of boxes:

$$\text{PageIoU}(P, G) = \frac{\sum_{p \in \Omega} M_P(p) M_G(p)}{\sum_{p \in \Omega} \mathbf{1}[M_P(p) + M_G(p) > 0]}. \quad (4)$$

Label PageIoU. Let $c(g)$ and $c(b)$ be class labels. We build pixel-wise label maps $L_G(p)$ and $L_P(p)$ by assigning each pixel the label of the *smallest-area* box covering it (background otherwise). Label PageIoU counts intersection only when labels agree:

$$\text{LabelPageIoU}(P, G) = \frac{\sum_{p \in \Omega} \mathbf{1}[L_P(p) = L_G(p) \wedge L_G(p) \neq \text{bg}]}{\sum_{p \in \Omega} \mathbf{1}[M_P(p) + M_G(p) > 0]}. \quad (5)$$

Recall@50. Let $\text{IoU}(b, g) = \frac{|b \cap g|}{|b \cup g|}$. A ground-truth box g is matched if there exists a prediction b with $\text{IoU}(b, g) \geq 0.5$ (and, for label-aware recall, $c(b) = c(g)$). We compute one-to-one matches greedily by prediction confidence. Then

$$\text{Recall}@50 = \frac{1}{|G|} \sum_{g \in G} \mathbf{1}[g \text{ is matched}]. \quad (6)$$

PixCov (pixel coverage). For datasets with sparse target annotations (e.g., ScreenSpot), we report pixel coverage of the annotated target area:

$$\text{PixCov}(P, G) = \frac{\sum_{p \in \Omega} M_P(p) M_G(p)}{\sum_{p \in \Omega} M_G(p)}. \quad (7)$$

mAP@50. We compute label-aware mAP@50 with one-to-one greedy matching at $\text{IoU} \geq 0.5$ (same-class), rank predictions by confidence when available (otherwise use score = 1.0), and average AP over classes present in the ground truth:

$$\text{mAP}@50 = \frac{1}{|\mathcal{C}^+|} \sum_{k \in \mathcal{C}^+} \text{AP}_k@50, \quad (8)$$

where $\mathcal{C}^+ = \{k \in \mathcal{C} \mid |G_k| > 0\}$ denotes classes that appear in the ground truth.

7.4. Additional Results

This section includes supplementary tables and ablations referenced in the main paper.

Table 9. Ablation on foundation VLMs finetuning with ScreenParse. We report results on ScreenParse, GroundCUA, and ScreenSpot (Web/PC/Mobile splits). Recall denotes class-agnostic Recall@50 and PixCov denotes PageIoU recall.

Model	Size	ScreenParse			GroundCUA		ScreenSpot (Web)		ScreenSpot (PC)		ScreenSpot (Mobile)	
		Page IoU	Label Page IoU	mAP@50	Page IoU	Label Page IoU	Recall	PixCov	Recall	PixCov	Recall	PixCov
InternVL3-2B	2B	0.116	0.030	0.000	0.025	0.006	0.002	0.057	0.018	0.109	0.068	0.321
InternVL3-2B + ScreenParse	2B	0.497 (+0.381)	0.155 (+0.125)	0.063 (+0.063)	0.203 (+0.178)	0.036 (+0.030)	0.172 (+0.170)	0.592 (+0.535)	0.081 (+0.063)	0.628 (+0.519)	0.100 (+0.032)	0.527 (+0.206)
Qwen3-VL-2B-Instruct	2B	0.228	0.051	0.023	0.030	0.005	0.232	0.292	0.171	0.218	0.143	0.250
Qwen3-VL-8B-Instruct	8B	0.281	0.043	0.000	0.060	0.010	0.229	0.346	0.201	0.300	0.193	0.311
Qwen3-VL-2B-Instruct + ScreenParse	2B	0.585 (+0.357)	0.166 (+0.115)	0.152 (+0.129)	0.090 (+0.060)	0.019 (+0.014)	0.477 (+0.245)	0.720 (+0.428)	0.201 (+0.030)	0.443 (+0.225)	0.108 (-0.035)	0.477 (+0.227)

7.5. Qualitative Results

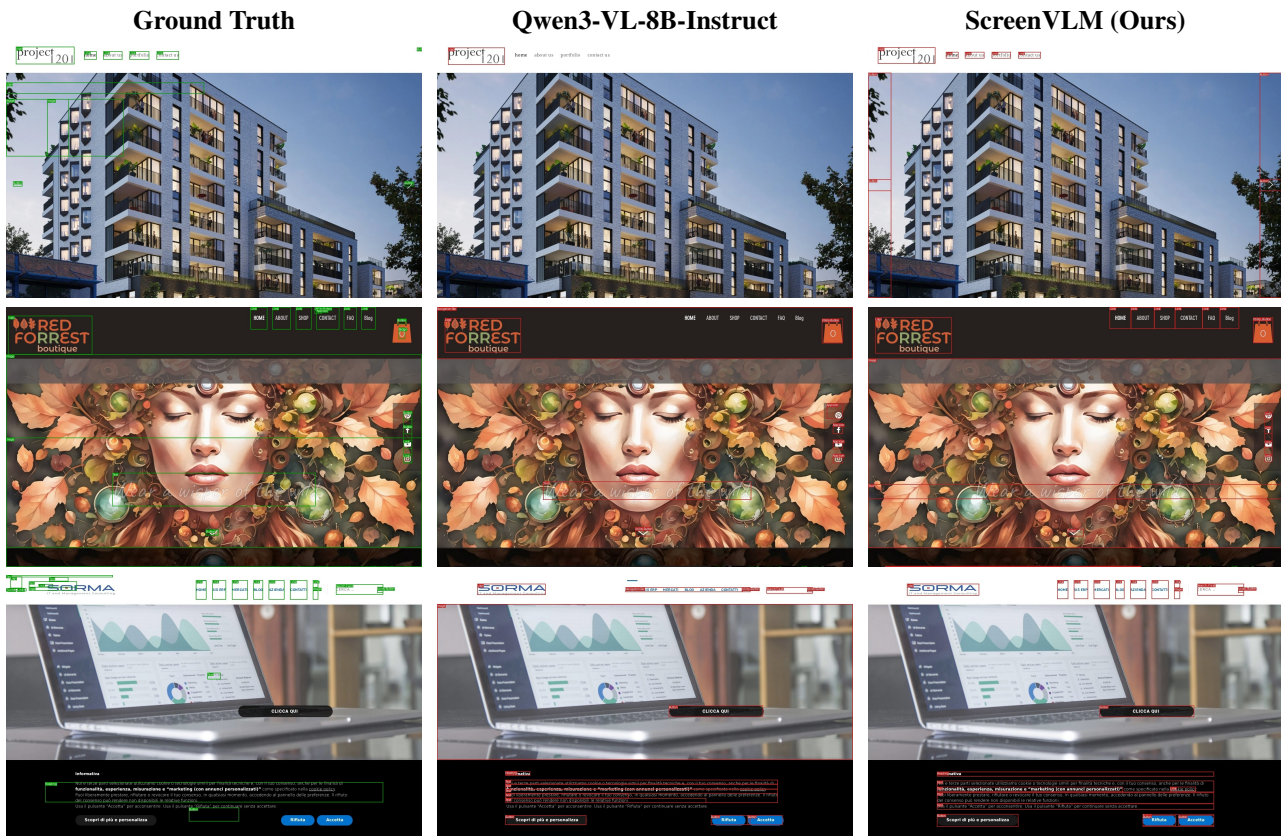


Figure 6. Qualitative screen parsing predictions for VLMs. Each row shows the same screenshot across columns; bounding boxes and labels are rendered as overlays. As it can be seen, in terms of recall, localization and granularity of the predictions, our ScreenVLM model outperforms the Qwen3-VL-8B-Instruct model significantly. Some of the ground truth annotations contain errors due to the rendering or DOM extraction issues.

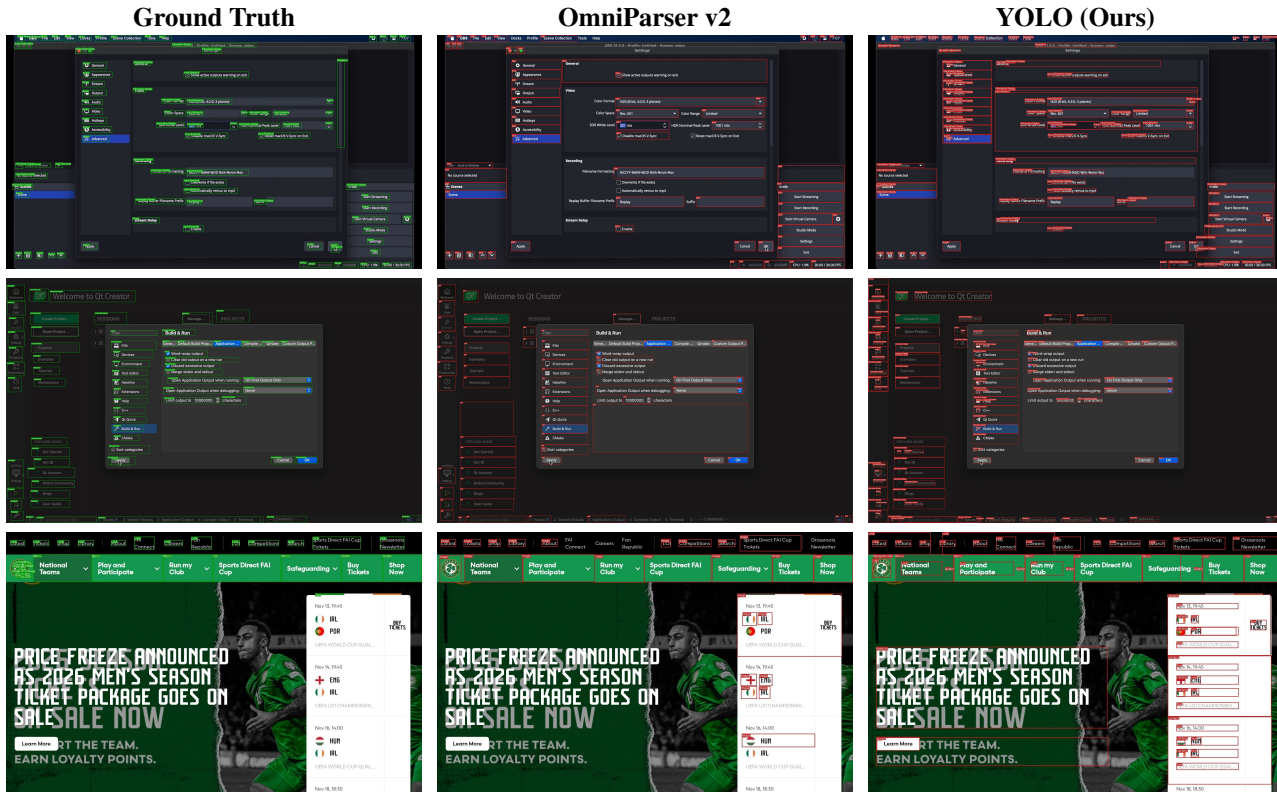


Figure 7. Qualitative screen parsing predictions for detector/parser baselines on GroundCUA dataset. Each row shows the same screenshot across columns. Our YOLO model has much less false negatives compared to OmniParser v2, and it covers text areas that may be important for understanding the UI.

ScreenParse

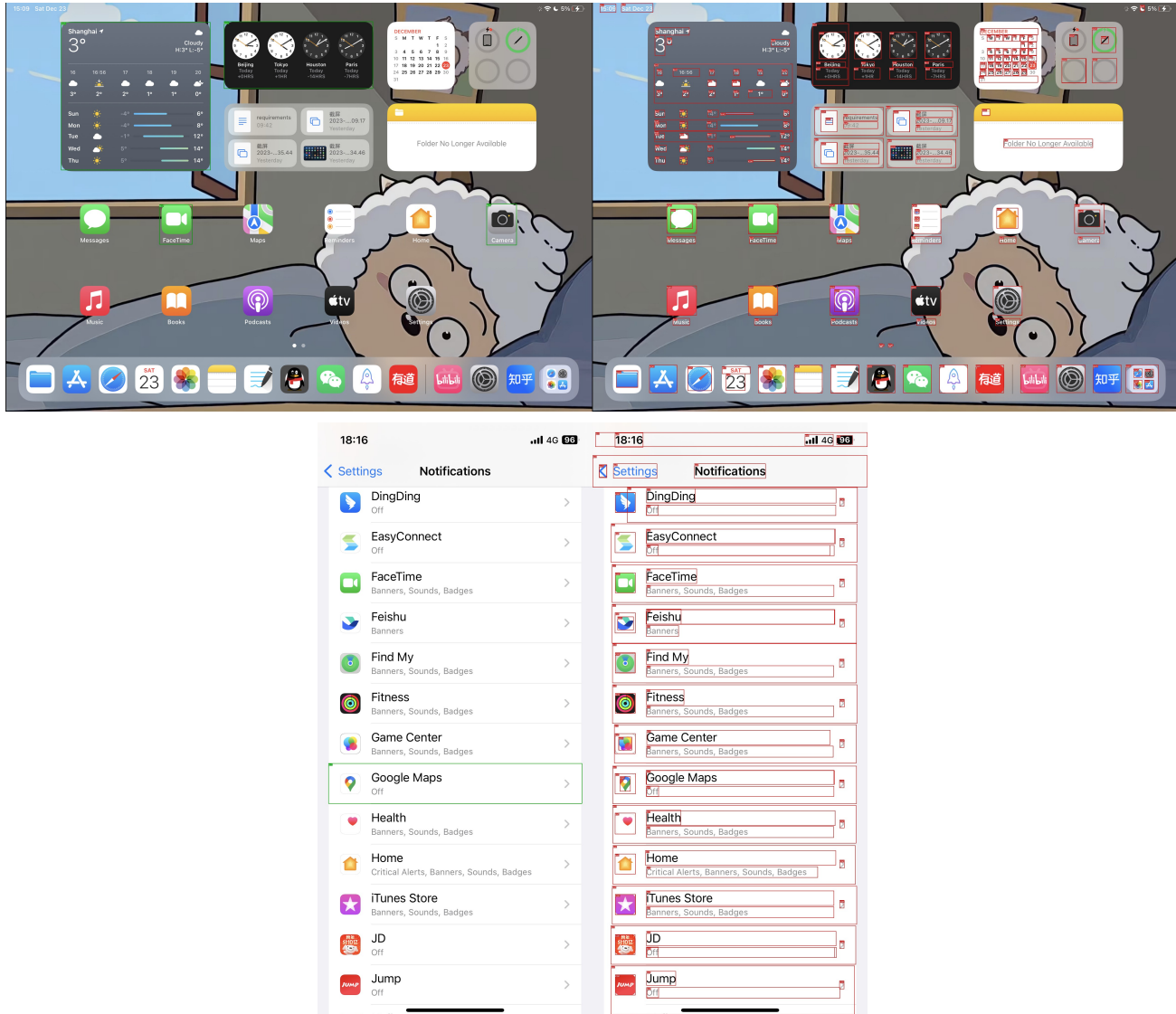


Figure 8. Out-of-distribution qualitative results of our YOLO model on the ScreenSpot *Mobile* split. Each visualization shows ground truth (left) and the model prediction (right). The ground truth visualization is not complete since ScreenSpot provides sparse annotations.

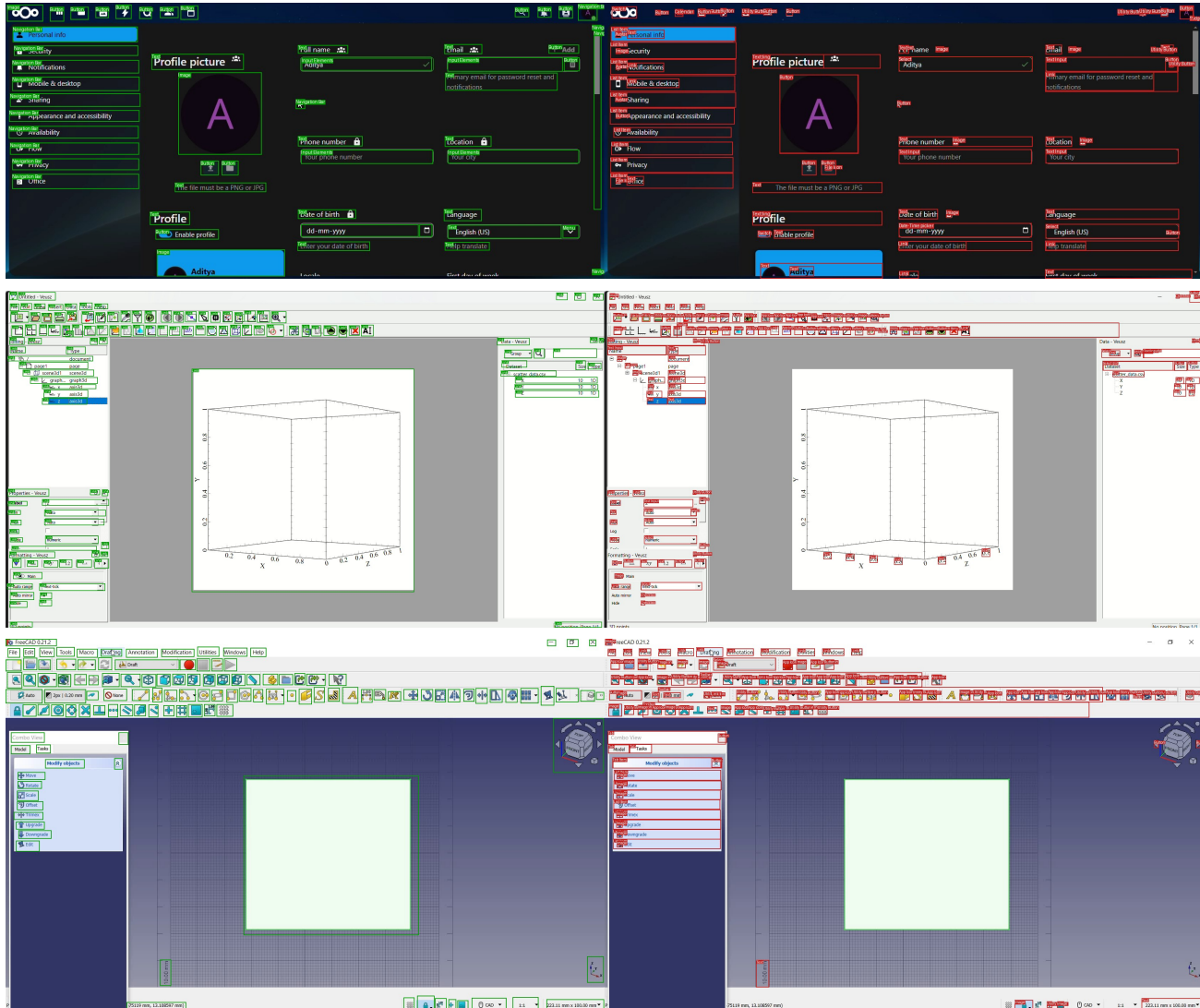


Figure 9. Out-of-distribution qualitative results of our YOLO model on the GroundCUA dataset. Each visualization shows ground truth (left) and the model prediction (right).



Figure 10. Additional qualitative results on ScreenSpot (PC). We compare OmniParser v2 against OmniParser v2 fine-tuned on ScreenParse.

ScreenParse

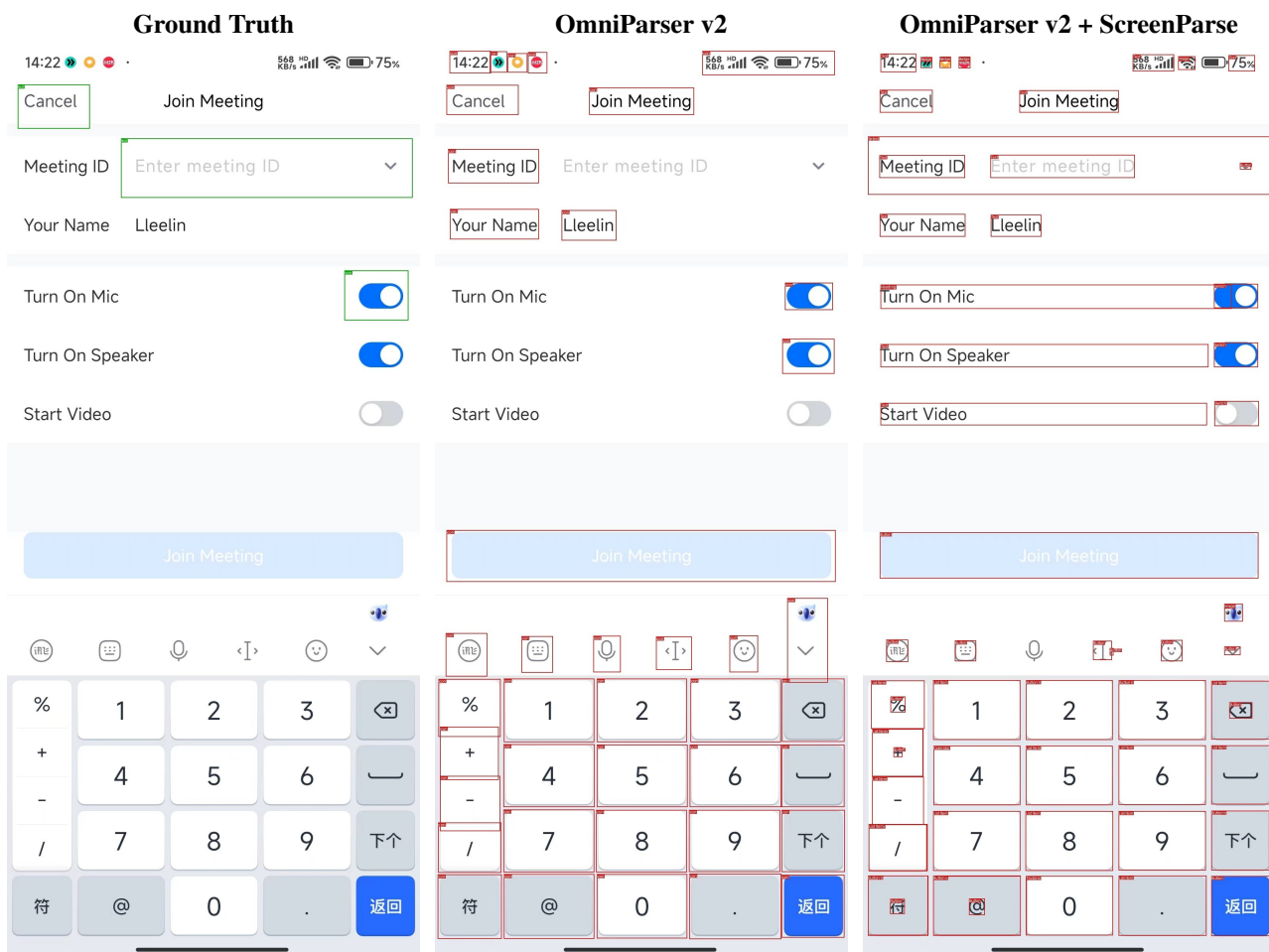


Figure 11. Additional qualitative result on ScreenSpot (Mobile): OmniParser v2 vs. OmniParser v2 fine-tuned on ScreenParse.

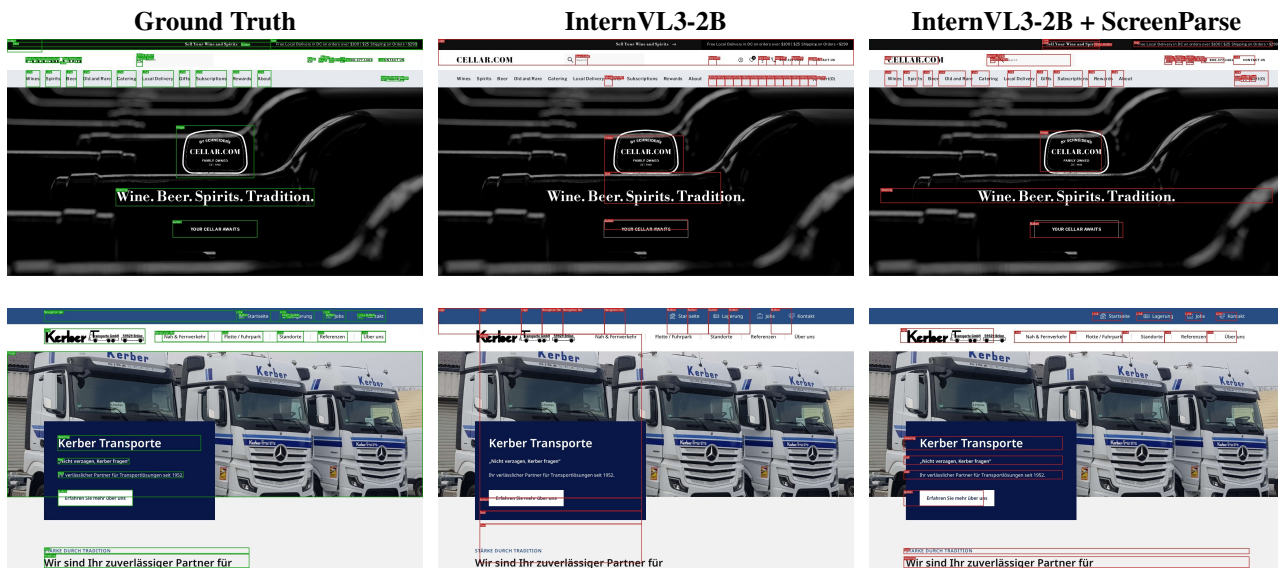


Figure 12. Additional qualitative results on ScreenParse: InternVL3-2B before and after fine-tuning on ScreenParse.

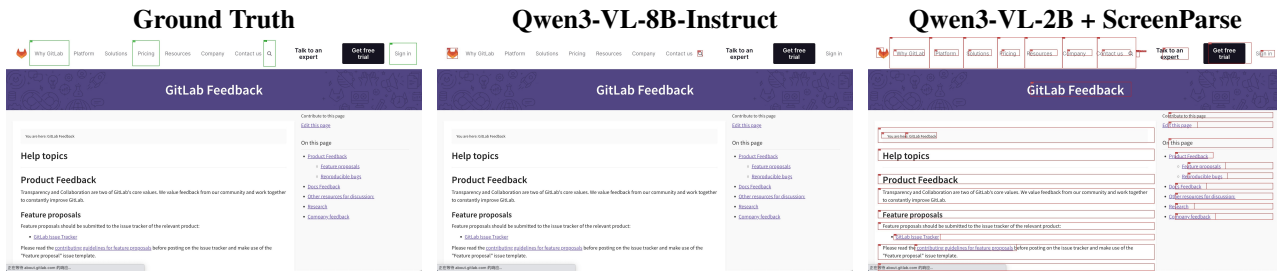


Figure 13. Additional qualitative result on ScreenSpot (Web): prompted Qwen3-VL-8B vs. Qwen3-VL-2B fine-tuned on ScreenParse.



Figure 14. Additional qualitative result on ScreenParse: OmniParser v2 before and after fine-tuning on ScreenParse.

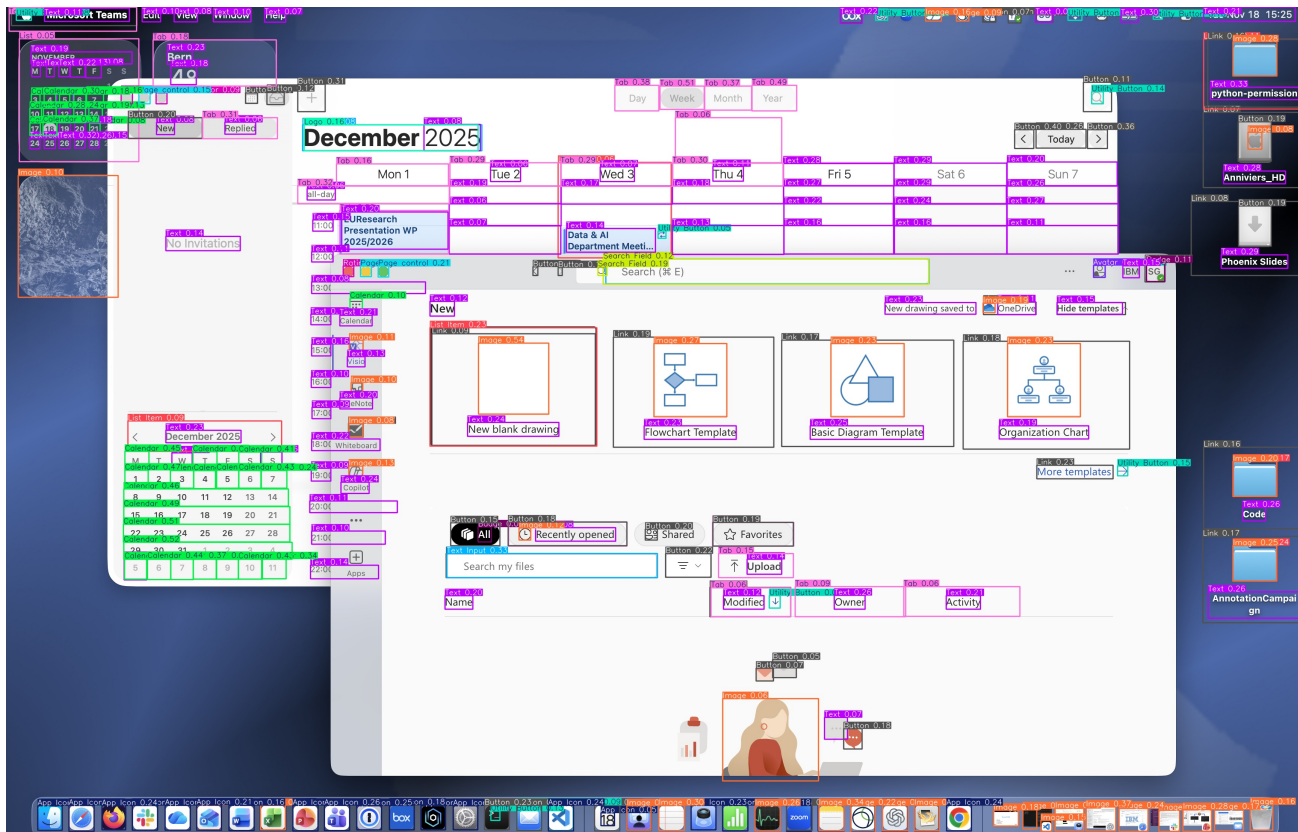


Figure 15. Out-of-distribution qualitative result of our YOLO detector on a complex desktop multi-window screen.

7.6. Webshot Pipeline Specifications

7.6.1. RENDERING AND SCREENSHOT STANDARDIZATION

Controlled rendering setup. All pages are rendered in a standardized browser environment (Chromium via Playwright) with viewport size of 1440 width and 900 height. We disabled CSS animations/transitions to avoid transient states and inconsistent layouts across runs. We use a bounded navigation timeout of **30s** and allow a short post-load settling period (**800ms**) before extracting annotations.

Viewport-only capture (default). By default, we capture the *top-of-page viewport* without scrolling. This makes the definition of “visible UI elements” unambiguous and avoids mixing content from multiple scroll positions into a single example. A full-page mode (with controlled scrolling to trigger lazy-loading) is supported, but ScreenParse is constructed under viewport-only capture for consistency.

7.6.2. DENSE UI ELEMENT EXTRACTION WITH DOM HIERARCHY

Element set and geometry. For each rendered page, we extract a set of UI elements by traversing the DOM and keeping elements that are inside the viewport. For each retained element we record: (i) its bounding box in pixel coordinates, (ii) a coarse element type inferred from HTML/ARIA cues (used as a fallback label prior to refinement), and (iii) its textual content (from on-page text, with optional OCR fallback; §7.6.3). We also record auxiliary metadata such as the accessibility tree snapshot for potential downstream use.

Hierarchy preservation. A core goal of ScreenParse is to represent screens as structured states rather than flat sets of boxes. We therefore preserve *parent-child* relationships induced by the DOM: each element stores its parent index and a list of children indices (restricted to the extracted visible set). This yields a tree/forest structure that captures containment and grouping (e.g., a navigation bar containing tabs and buttons), which enables hierarchical serialization (ScreenTag; §7.6.5) and training objectives beyond single-element grounding.

Multi-frame (iframe) handling. Web pages often embed content in iframes. We extract elements from the main frame as well as embedded frames, and map their coordinates into a shared page coordinate system so that all boxes are comparable and can be jointly serialized.

7.6.3. TEXT EXTRACTION AND OCR

Fine-grained text boxes. In addition to per-element text, we optionally extract fine-grained text spans by collecting bounding rectangles of rendered text. This supports richer supervision and analysis (e.g., separating layout regions from text density).

OCR fallback (optional). When enabled and available, we run OCR (Tesseract) over element crops to fill missing or unreliable text for elements whose DOM text is empty (common for canvas-based or heavily scripted UIs). OCR is used as a fallback signal; DOM text remains primary when present.

7.6.4. FILTERING AND SAMPLE VALIDATION

Raw DOM extraction is intentionally dense and contains noise (layout wrappers, invisible artifacts, redundant overlapping boxes). We apply conservative filters designed to improve label quality while retaining semantically important UI.

Geometric and visibility filtering. We remove elements that are clearly unsuitable training targets, including: (i) invalid boxes (non-positive width/height), (ii) boxes that are almost entirely outside the viewport or have negligible visible overlap, (iii) *tiny* artifacts with area < 4 pixels² (unless the element is recognized as an important interactive type), and (iv) overly large boxes that behave like page-wide wrappers (we set maximum area to **50%** of the viewport area during crawling, with a special-case exception for image regions).

Duplicate suppression. To reduce redundant annotations, we suppress near-duplicate boxes using IoU-based overlap checks with a threshold of **0.95**. When duplicates are detected, we preferentially keep boxes corresponding to interactive/semantically meaningful element types. To reduce redundancy at dataset level, we provide an hash based near-duplicate filter

with default Hamming radius **8**.

7.6.5. SCREENTAG SERIALIZATION

We represent each screen in a compact structure we called (**ScreenTag**) to serve as an efficient dense parsing target. Each element is serialized as a typed tag with discretized location tokens:

```
<tag><x_1><y_1><x_2><y_2> text children </tag>,
```

where coordinates are given in left, top, right, bottom order and normalized to a **grid of 0-500**. We traverse the hierarchy depth-first and order siblings by top-left position to encourage stable reading order.

Vocabulary and Tokenization. To make structured generation efficient, we extend the tokenizer vocabulary with *single* special tokens for the ScreenTags, including opening/closing tags for the 55 UI classes and discretized location tokens for each coordinate bin on the **0-500** grid. This avoids producing tag strings as multi-token fragments, reduces the effective sequence length, and makes generation more efficient.

Ground-truth cleanup. Before writing labels, we apply an additional per-class duplicate cleanup with thresholds **IoU** > 0.65 and (for non-nestable classes such as Text/Button/Image) a containment-based duplicate rule with threshold **0.65**. For container-like classes we keep the largest box in a duplicate cluster; for atomic elements we keep the smallest.

The code for the Webshot pipeline will be released.

7.7. VLM-as-a-Judge Prompt for Annotation Quality Filtering

In the Webshot pipeline, we use qwen3-VL-8B-instruct as a VLM-as-a-judge to score screen annotations and filter low-quality pages in ScreenParse. The threshold chosen is 0.70 to filter bad samples. The system and user prompts are provided below:

VLM-as-a-Judge Prompt (Qwen3-VL-8B-Instruct)

```
_QUALITY_SYSTEM_PROMPT = '''You are a rigorous judge of UI bounding-box annotations.
```

You will be given:

- ONE image: a screenshot of a user interface with bounding boxes and text labels drawn on top of it. Each box corresponds to a single annotated UI element.
- The labels near the boxes show the element class (for example: Text, Button, Link, Image, Navigation Bar, etc.).

Your task is to evaluate ****only the quality of the bounding box annotations****, NOT the correctness of the class names.

When judging, ****treat the class label text as low priority****:

- Assume the class labels are mostly correct.
- Only use the labels to distinguish boxes or understand their intent.
- Do NOT heavily penalize minor class mistakes (e.g., Text vs Heading).
- Focus on: "Is there a sensible box here?" and "Are obvious UI elements missing or duplicated?"

EVALUATION DIMENSIONS

You must score the annotation quality using **FOUR** sub-scores and **ONE** overall score.

All scores are from 0 to 100, where:

- 100 = perfect in that dimension
- 80-99 = very good, only minor issues
- 60-79 = usable, but several noticeable issues
- 40-59 = poor, many issues
- 0-39 = extremely bad

1) COVERAGE / MISSING ELEMENTS (0-100)

- Look for visually obvious, distinct UI elements that **should** be annotated:
 - buttons, main text blocks, headings, input fields, icons, major images, cards, menu items, etc.
 - Large and important items that should be covered:
 - main hero images, large central text, clearly clickable buttons or tabs, prominent fields.
 - Ignore tiny decorative details (small icons, background textures) unless they clearly look like clickable controls.
 - Don't forget that we are referring to the ui elements and text coverage, if there are empty areas, white/blank parts of the screen, it is correct that there shouldn't be boxes there.
 - High score (90-100): Almost every clear, medium-to-large UI element has a box.
 - Medium score (60-80): Some obvious UI elements are missing (e.g., a few main buttons or text blocks are unannotated).
 - Low score (<60): Many large, obvious UI elements have NO bounding boxes.

2) FALSE POSITIVES / SPURIOUS BOXES (0-100)

- Penalize boxes that are not aligned with any visible UI element, such as:
 - Boxes in completely blank areas.
 - Boxes that repeat the same position but shifted somewhere else on the screen where nothing exists.
 - Boxes over pure background images or whitespace where there is no clear object or control.
- Do NOT treat "container + child" as false positive if the container corresponds to a real region (e.g., window, navbar, card) and the child is a real button or text.
- High score (90-100): Almost all boxes correspond to real UI elements or meaningful regions.
- Medium score (60-80): Some boxes are obviously floating over empty space or nonsense regions.
- Low score (<60): Many boxes are on empty background, duplicated far from any element, or clearly not aligned with any UI structure.

3) DUPLICATION / REDUNDANCY (0-100)

Focus especially on SAME-CLASS duplications:

- For NON-NESTABLE classes (for example: Text, Heading, Button, Checkbox, Radiobox, Switch, Slider, Text Input, Search Field, Image, Logo, Icon, etc.):
 - Two boxes of the same class that heavily overlap OR where one box is completely inside another usually indicate a problem.
 - Examples of bad cases:
 - A "Text" box entirely inside another "Text" box for the same text block.
 - A button annotated two or three times with slightly shifted boxes around the same visual button.
- For container vs child classes (for example: Window + Button, Navigation Bar + Text, Card + Image):
 - It is OK for a container and its children to overlap (this is NOT a duplication).
- High score (90-100): Almost no obviously redundant same-class boxes; each UI element is annotated once.
- Medium score (60-80): Some elements appear to have 2 overlapping same-class boxes.
- Low score (<60): Many same-class boxes stacked or nested on top of each other in the same location, especially for Text and Button.

4) LOCALIZATION / ALIGNMENT (0-100)

- Evaluate how well each bounding box fits its intended UI element.
- Good annotation:
 - The box tightly covers the element, with small margins.
 - It does not cut off major parts of the element.
- Penalize:

- Boxes that are much larger than the element and include large amounts of unrelated background.
- Boxes that cut off significant parts of the text/button/icon.
- High score (90-100): Boxes match element boundaries closely.
- Medium score (60-80): Some boxes are too loose or slightly misaligned, but the element is still clear.
- Low score (<60): Many boxes are badly misaligned, cutting off elements or covering very wrong region sizes.

OVERALL SCORE

Combine the four dimensions into a single ****overall_quality**** score (0-100). Use approximately this weighting:

- Coverage / Missing: 40%
- False Positives: 25%
- Duplication: 20%
- Localization: 15%

Guidance:

- 90-100: Excellent annotation; safe to use as high-quality training data.
- 70-89: Good annotation; usable without manual review.
- 50-69: Borderline; has significant issues, might be filtered out if we want very clean data.
- 0-49: Bad annotation; should be excluded.

SPECIAL FAILURE PATTERNS TO PENALIZE HARD

Please penalize strongly when you see:

- Repeated "ghost" boxes:
The same bounding box shape appears multiple times in unrelated places in the screenshot (especially when those copies are not aligned with any visible element). This is a strong indicator of broken coordinates.
- Repeated same-class boxes over one element:
For example, several "Text" labels stacked over the same text string, or multiple overlapping "Button" boxes for one button.
- Missing entire regions:
For example, a large hero image, main headline, or obvious call-to-action button with no annotation at all.
- Small irrelevant repeated boxes:
Many tiny boxes of the same class (for example, small "Icon" or "Image" boxes) scattered around the screenshot that do not correspond to any real UI elements.

When such failure patterns are frequent across the image, the ****overall_quality**** should usually be below 40.

OUTPUT FORMAT

Return your answer as ****pure JSON****, with no extra commentary.

Use this schema:

{

```

"short_summary":           "<one-line summary of annotation quality, e.g. 'Good
                           coverage but many duplicate Text boxes in irrelevant areas'>",
"coverage_score":          "<number 0-100>,
"false_positive_score":    "<number 0-100>,
"duplication_score":      "<number 0-100>,
"localization_score":     "<number 0-100>,
"overall_quality":        "<number 0-100>
}

Start with "short_summary" first - briefly describe the main quality issues (or lack
thereof) before scoring.

Do not include any other keys or text outside this JSON.''

```

`_QUALITY_USER_PROMPT = "Please evaluate the annotation quality of this visualization
image."`

7.8. VLM Prompt for Class Refinement

We refine each element into the ScreenTag label set with a VLM that sees the entire page screenshot, the element crop, and a compact HTML/ARIA snippet. The following prompts map each element to a single class and an interactability flag.

System prompt.

Class Refinement System Prompt

You classify ONE UI element using:
 (1) the full-page screenshot,
 (2) a cropped image of the element,
 (3) a compact HTML-like snippet for the element.

Labeling rule:

- Choose exactly ONE label from the allowed list.
- Prefer the most specific, functionally correct label that best matches the element's purpose in its context.
- Favor function over appearance. If a more specific option exists, prefer it (e.g., "Search Field" over "Text Input" when it is clearly a search box; "Link" over "Text" if it navigates; "Button" over "Image" if it acts like a button).
- Use HTML/ARIA (role, type, href, aria-*, classes) to break ties. If still ambiguous, choose the closest single label from the list.

Interactability:

- Set interactable=true if a typical end-user can directly act on this element itself (click/tap/select/type/drag/scroll within it). Otherwise false (pure content/decoration or a passive container).

Output ONLY one JSON object on a single line:
`{"label": "<one-of-allowed>","interactable": <true|false>}`

User prompt template.

Class Refinement User Prompt Template (55-class ScreenTag)

Allowed labels:
 - Table
 - Column/Browser
 - Button
 - Utility Button
 - App Icon
 - Navigation Bar

- Status Bar
- Search Field
- Toolbar
- Tooltip
- Video
- Tab Bar
- Side Bar
- Slider
- Picker
- ContextMenu
- DockMenu
- EditMenu
- Image
- Scroll
- Switch
- File Icon
- Chart
- Window
- Screen
- List
- List Item
- PopUp Menu
- Steppers
- Toggles
- Text Input
- Rating Indicator
- Checkbox
- Radiobox
- Select
- Avatar
- Badge
- Alert
- Progress bar
- Bottom navigation
- Breadcrumb
- Page control
- Link
- Menu
- Pagination
- Tab
- Search Bar
- Date-Time picker
- Calendar
- Text
- Heading
- Code snippet
- Carousel
- Notification
- Logo

Element HTML snippet:

```
<HTML_SNIPPET>
```

Instructions:

- Consider the crop FIRST to understand the element's visual identity.
- Use the full-page screenshot for surrounding context and function.
- Use HTML attributes (tag, role, type, aria-*, classes) as semantic hints.
- Output strictly one JSON object as specified (no extra text).

7.9. VLM Inference Prompts for Evaluation

For prompting-based baselines, we ask the model to extract all visible UI elements and return a JSON list with normalized bounding boxes, labels, and visible text. We use dataset-specific label sets: the 55-class ScreenTag taxonomy for ScreenParse (Tab. 8), the 8-class GroundCUA schema, and the 2-class ScreenSpot schema.

Qwen3-VL and InternVL3 Inference Prompt

You are a UI parser. Given a screenshot image, extract all visible UI elements.
Return JSON list with objects:
{ "bbox_ltrb": [l, t, r, b], "label": "<type>", "text": "<visible text>" }.
The bbox_ltrb should be normalized to 0-1000. (l, t, r, b). Include all elements.

Allowed labels (ScreenParse / ScreenTag-55): [see Table 8]

Allowed labels (GroundCUA-8) :

- Input Element
- Sidebar
- Information Display
- Button
- Navigation
- Visual Elements
- Menu
- Others

Allowed labels (ScreenSpot-2) :

- icon
- text